Geomorphology of Ma'adim Vallis, Mars, and associated paleolake basins

Rossman P. Irwin III
Center for Earth and Planetary Studies, National Air and Space Museum, Smithsonian Institution, Washington, DC, USA
Department of Environmental Sciences, University of Virginia, Charlottesville, Virginia, USA

Alan D. Howard
Department of Environmental Sciences, University of Virginia, Charlottesville, Virginia, USA

Ted A. Maxwell
Center for Earth and Planetary Studies, National Air and Space Museum, Smithsonian Institution, Washington, DC, USA

Received 27 April 2004; revised 7 October 2004; accepted 26 October 2004; published 30 December 2004.

[1] Ma'adim Vallis, one of the largest valleys in the Martian highlands, appears to have originated by catastrophic overflow of a large paleolake located south of the valley heads. Ma'adim Vallis debouched to Gusev crater, 900 km to the north, the landing site for the Spirit Mars Exploration Rover. Support for the paleolake overflow hypothesis comes from the following characteristics: (1) With a channel width of 3 km at its head, Ma'adim Vallis originates at two (eastern and western) gaps incised into the divide of the $\sim$1.1 M km^2 enclosed Eridania head basin, which suggests a lake as the water source. (2) The sinuous course of Ma'adim Vallis is consistent with overland flow controlled by preexisting surface topography, and structural control is not evident or required to explain the valley course. (3) The nearly constant $\sim$5 km width of the inner channel through crater rim breaches, the anastomosing course of the wide western tributary, the migration of the inner channel to the outer margins of bends in the valley's lower reach, a medial sedimentary bar $\sim$200 m in height, and a step-pool sequence are consistent with modeled flows of $1-5 \times 10^6$ m^3/s. Peak discharges were likely higher but are poorly constrained by the relict channel geometry. (4) Small direct tributary valleys to Ma'adim Vallis have convex-up longitudinal profiles, suggesting a hanging relationship to a valley that was incised quickly relative to the timescales of tributary development. (5) The Eridania basin had adequate volume between the initial divide and the incised gap elevations to carve Ma'adim Vallis during a single flood. (6) The Eridania basin is composed of many overlapping, highly degraded and deeply buried impact craters. The floor materials of the six largest craters have an unusually high internal relief ($\sim$1 km) and slope ($\sim$0.5–1.5°) among degraded Martian craters, which are usually flat-floored. Long-term, fluvial sediment transport appears to have been inhibited within these craters, and the topography is inconsistent with basaltic infilling. (7) Fluvial valleys do not dissect the slopes of these deeper crater floor depressions, unlike similar slopes that are dissected at higher levels in the watershed. These characteristics (6, 7) suggest that water mantled at least the lower parts of the Eridania basin floor throughout the period of relatively intense erosion early in Martian history. The lake level increased and an overflow occurred near the close of the Noachian (age determined using >5 km crater counts). Initially, the Eridania basin debouched northward at two locations into the intermediate basin, a highly degraded impact crater $\sim$500 km in diameter. As this intermediate basin was temporarily filled with water, erosion took place first along the lower (northern) reach of Ma'adim Vallis, debouching to Gusev crater. The western overflow point was later abandoned, and erosion of the intermediate basin interior was concentrated along the eastern pathway. Subsequent air fall deposition, impact gardening, tectonism, and limited fluvial erosion modified the Eridania basin region, so evidence for a paleolake is restricted to larger landforms that could survive post-Noachian degradation processes. *INDEX TERMS:* 6225 Planetology: Solar

0148-0227/04/2004JE002287$09.00

System Objects: Mars; 5415 Planetology: Solid Surface Planets: Erosion and weathering; 1824 Hydrology: Geomorphology (1625); 1821 Hydrology: Floods; *KEYWORDS:* flood, lake, valley networks

Citation: Irwin, R. P., III, A. D. Howard, and T. A. Maxwell (2004), Geomorphology of Ma'adim Vallis, Mars, and associated paleolake basins, *J. Geophys. Res.*, *109*, E12009, doi:10.1029/2004JE002287.

1. Introduction

[2] The discovery of large outflow channels and valley networks on Mars during the 1971–72 Mariner 9 mission [*McCauley et al.*, 1972; *Milton*, 1973] suggested that Mars once had abundant surface water, much of which is still present as polar and ground ice (summarized by *Carr* [1996]). Pressure-driven groundwater originating from fractures or chaotic terrain appears to have formed most of the outflow channels in the Chryse region of Mars [*Carr*, 1979], but several wide, deeply incised highland valleys do not exhibit chaotic terrain at their source. Some of these larger highland valleys occupy ridge-bounded drainage basins and have tributary networks of small valleys, suggesting formation by fluvial runoff and/or groundwater sapping [*Sharp and Malin*, 1975; *Grant*, 2000; *Irwin and Howard*, 2002; *Aharonson et al.*, 2002; *Hynek and Phillips*, 2003]. Other valleys originate at gaps incised into the drainage divides of large enclosed basins or impact craters, suggesting a water supply from overflowing paleolakes [*Goldspiel and Squyres*, 1991; *Cabrol and Grin*, 1999; *Clifford and Parker*, 2001]. The cratered highland landscape was favorable for ponding of water at many sites, but evidence for overflows (which would require high water tables or relatively abundant inflows) is less common. Overflow gaps originating above an undissected basin floor are, however, the most definitive evidence that paleolakes did occur on Mars, particularly in basins where other surface features support this conclusion. Paleolakes could be favorable sites for hosting and preserving evidence of former life, if it existed on Mars [e.g., *Cabrol and Grin*, 1999], so a thorough characterization of these sites is beneficial for targeting future human and robotic exploration.

[3] At 8–25 km wide, Ma'adim Vallis in Terra Cimmeria (Figure 1) is similar in size to the outflow channels, but it formed earlier than did most of the large valleys on Mars [*Masursky et al.*, 1977, 1980; *Carr and Clow*, 1981] and contemporary with small valley network activity near the Noachian/Hesperian boundary [*Irwin et al.*, 2002] (~3.7 Ga before present from *Hartmann and Neukum* [2001]). We previously concluded that Ma'adim Vallis was carved by an overflowing paleolake located immediately south of the valley head, on the basis of several lines of morphologic evidence [*Irwin et al.*, 2002] that are detailed and reinforced with new analysis in this paper. Alternative published hypotheses involve an outflow or long-term fluvial activity, perhaps with structural control of groundwater flows, and these concepts are also addressed here. While other process models may yet be developed for this or other features in the Martian landscape, we show that the available data is consistent with the origin of Ma'adim Vallis by paleolake overflow, followed by a limited period of fluvial activity to partially incise its tributary network. We identify the features that can be used to identify a source paleolake in this region, we describe the rapid development of Ma'adim Vallis during a catastrophic overflow, and we constrain the magnitude of the flood. The morphology of Ma'adim Vallis and its tributary valleys is also provided as evidence for a paleolake overflow. These observations provide an integrated history of the Eridania basin, Ma'adim Vallis, and Gusev crater; offering a set of features that may be used to recognize paleolakes elsewhere on Mars. This study has direct relevance to the Mars Exploration Rover (MER) mission, as Gusev crater is the landing site for the Spirit rover [*Golombek et al.*, 2003; *Grant et al.*, 2004].

1.1. Description and Terminology of the Ma'adim Vallis System

[4] Ma'adim Vallis is among the largest valleys on Mars, and it originates full-born, with an upstream inner channel width nearly equal to its downstream dimensions (use of the term "channel" is justified in section 4.2 in reference to the wide, commonly flat cross section of the valley floor). The inner channel is 2.5–4 km wide along a steep reach near the source, and a width of 3–5 km is common along lower-gradient reaches downstream. The overall length of the valley is 920 km, from the source northward to the Gusev crater rim entrance breach where the valley ends (Figure 1). The volume of Ma'adim Vallis and its tributaries, below the sharp break in slope at the top of the valley sidewalls, is ~14,000 km^3 [*Goldspiel and Squyres*, 1991; *Cabrol et al.*, 1996; *Irwin et al.*, 2002]. Transporting this volume of sediment would require at least 35,000 km^3 of water given *Komar*'s [1980] maximum possible water/sediment volume concentration of 0.4, or an order of magnitude larger water volume for more typical fluvial sediment concentrations.

[5] Incision of Ma'adim Vallis connected three originally enclosed basins, (1) the Eridania basin (Figure 2); (2) the intermediate basin, a 500 km, highly degraded impact crater (Figure 1); and (3) Gusev crater at the valley terminus, in addition to several smaller craters that were breached. The divides of Gusev crater and the Eridania basin are only partially incised, so volumetrically reduced central basins still exist. In contrast, the northern divide of the intermediate basin was downcut to below its floor level, opening the basin completely for through-flowing drainage. The contiguous Ma'adim Vallis watershed network (not counting valleys in the Eridania basin watershed) occurs within the intermediate basin and on the northward-sloping intercrater plains between the intermediate basin and Gusev crater.

[6] Ma'adim Vallis originates ~25 km south of the breached intermediate basin rim within the enclosed, irregularly shaped Eridania basin (Figure 1). This large basin contains many highly degraded impact basins and craters on an otherwise near-level highland plateau (Figure 2). Within the eastern part of the Eridania basin, six deep subbasins (Gorgonum, Atlantis, Ariadnes and three unnamed basins) are highly degraded impact craters, where large segments of the crater rims are missing. The plains within these larger concave subbasins have up to 1.5 km of internal relief,

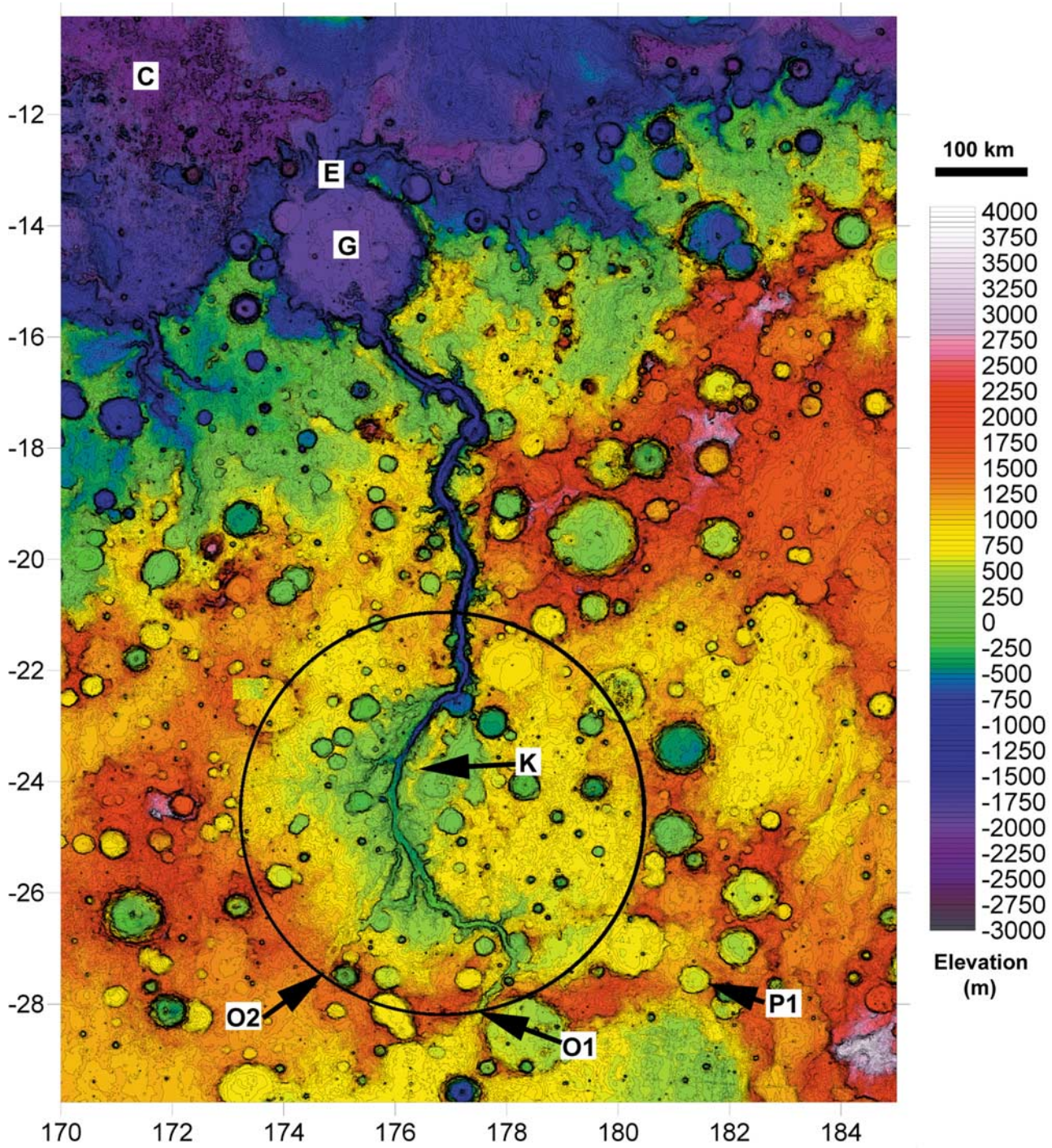

Figure 1. Ma'adim Vallis in a cylindrical projection of MOLA topography (128 pixel/degree, 50 m contour interval). The valley crosscuts a circular, highly degraded impact basin (black circle), identified as the intermediate basin. The locations of the knickpoint (K), Gusev crater (G), the Gusev exit breach (E), and chaotic terrain north of the valley terminus (C) are indicated. The lower reach of the valley lies north of the knickpoint, the intermediate reach extends along the rest of the intermediate basin floor, and the upper reach occurs along its southern interior slope. Ma'adim Vallis originates full-born at two source spillways (O1 and O2) in the intermediate basin divide. Another low point (P1) contains a degraded crater, the rim of which may have formerly raised the divide above the 1250 m level of O2.

unlike the nearly flat ridged plains and degraded crater floors that are common elsewhere on Mars. To the east and southeast of the Eridania basin, Newton and Copernicus craters also exhibit concave floors like the larger craters in the Eridania basin. We refer to the subaerial Eridania basin watershed separately from the paleolake basin itself. The watershed (using direct surface flow paths) typically extends only 10–100 km above the inferred paleolake

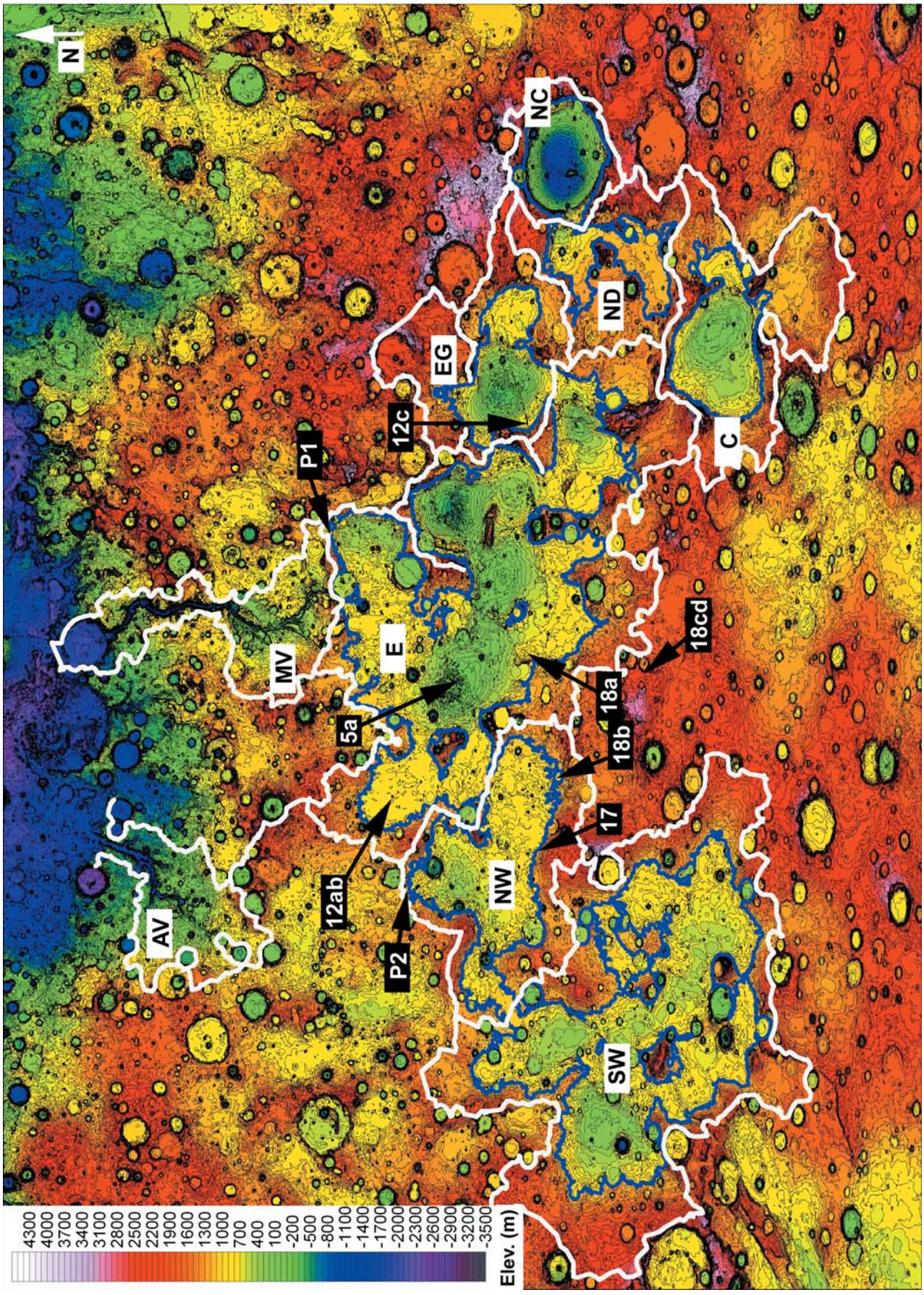
N
NC
ND
EG
12c
P1
C
MV
E
5a
18cd
18a
18b
17
12ab
AV
P2
NW
SW
Elev. (m)
4300
4000
3700
3400
3100
2800
2500
2200
1900
1600
1300
1000
700
400
100
-200
-500
-800
-1100
-1400
-1700
-2000
-2300
-2600
-2900
-3200
-3500

Figure 2

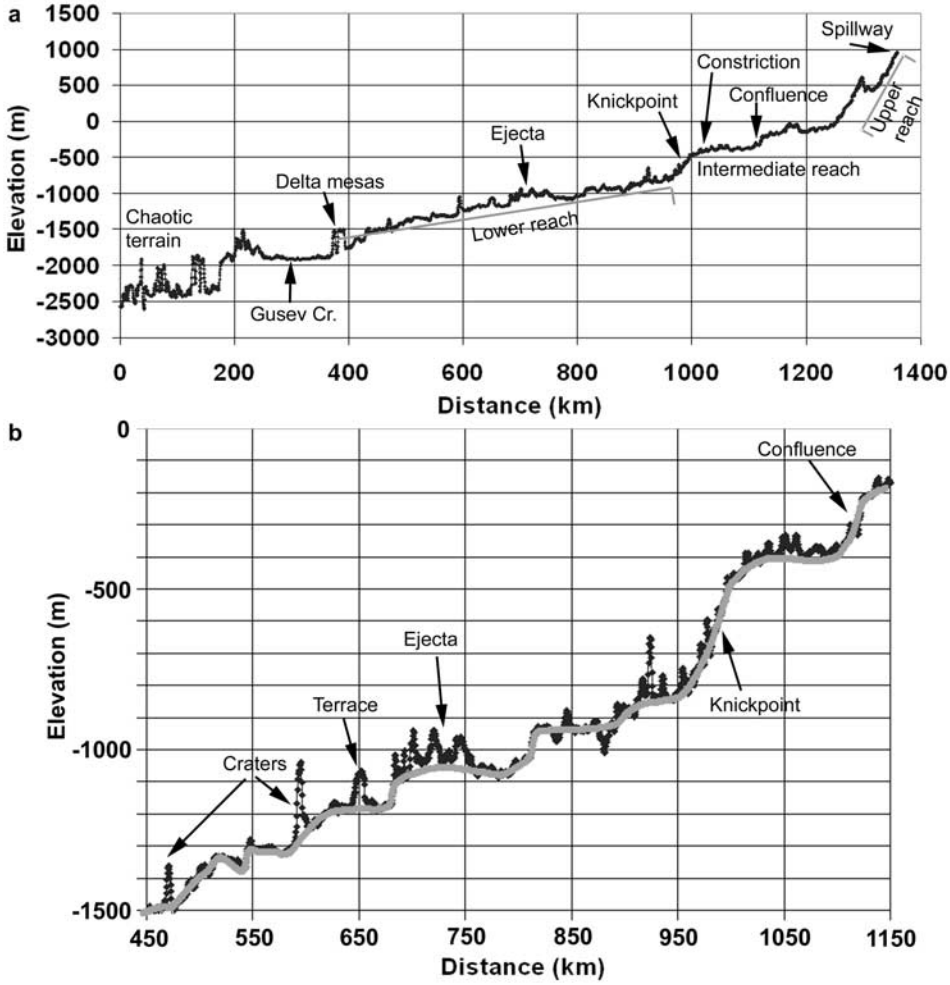

Figure 3. (a) Longitudinal profile of the main channel of Ma'adim Vallis from 128 pixel/degree MOLA topography. The steep upper reach of the channel transitions to the lower-gradient intermediate reach, where the large tributary meets the main valley. A constriction in the valley cross section and a knickpoint in the profile mark the location of a possible resistant outcrop. The Gusev crater paleolake had a level of −1,550 m and a depth of ∼400 m, suggested by the northern Gusev spillway and the elevation of mesas that are possible remains of a Ma'adim delta. Chaotic terrain development north of Gusev has obscured any evidence of flow into the lowlands. (b) Vertical exaggeration of the longitudinal profile of the lower reach and part of the intermediate reach, showing step-pool topography with pools up to tens of meters deep. The gray line approximates the inner channel thalweg.

highstand of 1100 to 1250 m. The Eridania basin and its watershed have a combined area of $\sim 2.08 \times 10^6$ km^2, not counting adjacent, low relief, topographically isolated crater or intercrater basins that may have contributed groundwater. The possible contributing area within a higher hydrologic divide surrounding the Eridania basin is $\sim 3 \times 10^6$ km^2.

[7] The longitudinal profile of Ma'adim Vallis (Figure 3) is subdivided into high- and low-gradient reaches. From the

Figure 2. MOLA topography of the Eridania basin and vicinity, in a cylindrical projection bounded by 10°S, 60°S, 140°E, and 210°E. The image is 2964 km from north to south. White lines are major drainage divides that delimit direct surface flow paths. The paleolake basin that supplied Ma'adim Vallis is contained within interconnected subbasins SW, NW, E, and EG. The blue line is the 1100 m contour, which approximately delimits the Eridania basin from its watershed. Around Newton Crater (NC) the blue line is the 1300 m contour, the (possibly unoccupied) overflow level for that basin. Drainage divides for small crater interiors and neighboring enclosed drainage basins are not shown. The drainage basins used for hypsometric analyses and crater counts are labeled with black letters: eastern subbasins (E + EG), eastern subbasin's Gorgonum Crater subset (EG), northwest subbasin (NW), southwest subbasin (SW), Newton Crater interior (NC), Newton Crater watershed (ND), Copernicus Crater and watershed (C), Ma'adim Vallis watershed (MV), and Al-Qahira Vallis watershed (AV, not used for hypsometry). The locations of high-resolution images of the Eridania basin used in subsequent figures are indicated with white numbers. Also in white numbers are the locations of undissected low points in the Eridania basin divide, P1 and P2, as discussed in the text.

eastern outlet, the steep upper reach of the valley descends from 950 m elevation into the intermediate basin interior. On the intermediate basin floor, the intermediate reach is wider and has a lower gradient than does the upper reach. This intermediate reach contains the confluence of the Ma'adim Vallis main channel and its anastomosing principal tributary, which originates at the western outlet of the Eridania basin. A prominent knickpoint with 300 m of relief separates the intermediate and lower reaches of the valley. As the lower reach leaves the intermediate basin, Ma'adim Vallis widens from ~10 to ~20 km, and terraces separate a wider outer valley from an inner channel that is similar in width to the intermediate and upper reaches of the valley. Despite local slope irregularities discussed in section 4.2, the lower reach maintains a nearly constant overall gradient of 0.0012 (0.07°) to the 160 km Gusev crater terminal basin, where mesas (which also record this channel gradient) at −1550 m may be remnants of a former delta [*Schneeberger*, 1989; *Grin and Cabrol*, 1997]. The northern rim of Gusev crater is also breached, so flows probably continued into the lowlands, but later chaotic terrain development and volcanism north of the crater precludes an evaluation of these possible flows.

1.2. Previous Investigations

[8] Ma'adim Vallis was first identified from Mariner 9 imaging in 1972, when it was referred to as the Rasena Channel, and several early papers considered its origin and age in the context of more general valley network studies [*Milton*, 1973; *Sharp and Malin*, 1975; *Malin*, 1976; *Masursky et al.*, 1977, 1980; *Carr and Clow*, 1981; *Brakenridge*, 1990; *Carr*, 1996]. *Sharp and Malin* [1975] provided the first detailed description of the valley and tributaries, noting the "irregularly constricted" reach of the channel that we now recognize as a knickpoint (Figure 3). They classified the valley as a runoff channel, which *Malin* [1976] supported by noting (as shown in section 3.2) that Ma'adim Vallis had attacked craters "through both grazing and head-on erosion." *Craddock et al.* [1987] used Viking Orbiter Infrared Thermal Mapper-derived thermal inertias to conclude that 0.25 to 0.5 mm aeolian sands had resurfaced the floor of Ma'adim Vallis, resulting in low rock abundances of <5%. This sediment transport was attributed to high-velocity valley winds [*Craddock et al.*, 1987], which have since been modeled and correlated with aeolian surface features in Gusev crater [*Greeley et al.*, 2003].

[9] In a significant advance, *Schneeberger* [1989] noted the mesas at the terminus of Ma'adim Vallis, where it debouches to Gusev crater, and suggested that the mesas may be eroded remnants of a delta that formed in a Gusev paleolake. This observation corrected the Mariner 9-based view that Ma'adim Vallis terminated in a 30 km crater, now recognized as two overlapping craters provisionally named New Plymouth and Downe, which are actually superposed on the Gusev crater rim and crosscut by the valley [*Landheim*, 1995; *Milam et al.*, 2003]. Subsequent base level declines within Gusev crater could be responsible for dissection of the former delta [*Schneeberger*, 1989; *Grin and Cabrol*, 1997]. *Goldspiel and Squyres* [1991] supported that interpretation, estimating that 13,000 km^3 of material had been eroded from Ma'adim Vallis and deposited in Gusev crater. *Carter et al.* [2001] have since compared the Mars Orbiter Laser Altimeter (MOLA) topography of Gusev to the younger Bakhuysen Crater, estimating that 15,100 km^3 of fill materials occur in Gusev. Prior to the Mars Global Surveyor (MGS) mission, depth and gradients in Ma'adim Vallis were calculated from atmospheric pressure [*Scott et al.*, 1978], shadows [*Lucchita and Dembosky*, 1994], digital elevation modeling from stereo images [*Thornhill et al.*, 1993a], and Earth-based radar [*Goldspiel et al.*, 1993]. *Thornhill et al.* [1993b] also used a shape-from-shading algorithm to calculate the discharge given arbitrary flow depths, which generated values from 10^4 to 10^6 m^3/s.

[10] More recently, *Landheim* [1995] suggested that Ma'adim Vallis is an outflow channel originating from etched and chaotic terrain located several hundred kilometers south of the valley head. Later episodes of flow were interpreted as possible but uncertain. Of the previous studies, the *Landheim* [1995] thesis bears the closest resemblance to the model we propose here, except that we invoke a paleolake rather than an outflow as the valley source for reasons described below, and details of the valley's incision history are now better defined with new topography. Cabrol and her colleagues have studied Ma'adim Vallis and Gusev crater in detail, and they have used their work to successfully advocate Gusev crater as a landing site for the first MER [*Cabrol et al.*, 1994; *Landheim et al.*, 1994]. In a series of papers [*Cabrol et al.*, 1996, 1997, 1998a, 1998b; *Grin and Cabrol*, 1997], they suggested that Ma'adim Vallis was supplied by groundwater or drainage from the chaotic terrain or Sirenum Fossae south of the valley head [see also *Landheim*, 1995; *Kuzmin et al.*, 2000; *Gulick*, 2001]. Crater counts suggesting a young surface mantle in Gusev crater, terraces within Ma'adim Vallis, and morphology of the terminal delta supported their view of a prolonged period of episodic activity spanning 0.7 to 2.0 Ga. They suggested that in this interval, impact craters twice interrupted Ma'adim Vallis, such that intravalley lakes formed at two sites. They attribute the terraces within Ma'adim Vallis to these ponding episodes and subsequent catastrophic flooding as the intravalley lakes were breached. They suggest that the morphology of the Gusev floor reflects the former paleolake [*Grin and Cabrol*, 1997], and that knobs in the floor are related to emergence of ice as pingoes [*Cabrol et al.*, 2000]. Our identification of an enclosed basin at the head of Ma'adim Vallis, a reevaluation of crater counts and new topographic data, and new detailed visible and thermal imaging of the valley cast much of that proposed history in doubt, as we describe herein. *Aharonson et al.* [2002] examined the irregular longitudinal profile of Ma'adim Vallis, noting that the valley and its tributary networks are poorly graded (they do not exhibit the usual downstream decline in gradient). This observation suggested that the drainage network was underdeveloped if formed by runoff erosion, and that it may be more consistent with sapping. *Aharonson et al.* [2002] plotted the valley head east of the location identified by *Scott et al.* [1978] and *Irwin et al.* [2002], which may have resulted from the superposition of a fresh crater on the upper reach of Ma'adim Vallis, which diverts a computationally derived flow path up an eastern tributary.

[11] Geologic maps at 1:5M scale were completed of the contributing drainage basins by *De Hon* [1977], *Scott et al.* [1978], *Mutch and Morris* [1979], and *Howard* [1979]. These earlier mappers recognized the dissected parts of the

landscape, eroded knobby and chaotic terrains, several units of smoother plains (some interpreted as volcanic), and aeolian mantles, but with variability in mapped units and interpretations. *Scott and Tanaka* [1986] and *Greeley and Guest* [1987] remapped the equatorial region of Mars at 1:15M scale, attributing the Eridania basin plains to volcanic resurfacing. *Kuzmin et al.* [2000] produced a detailed 1:500,000-scale map of geologic materials in and around Gusev crater, with interpretations similar to *Cabrol et al.* [1996, 1998a, 1998b]. *Milam et al.* [2003] remapped the Gusev floor using detailed MGS imaging and thermal inertia products, acknowledging a possible diversity of volcanic, fluvial, and aeolian materials in the crater.

2. Paleolake Indicators

[12] In this section, we describe the evidence for an extensive paleolake, based on the topography of the basin at the head of Ma'adim Vallis, the distribution and origin of erosional features within and around this basin, and the likely origin of the water.

2.1. Valley Head Morphology

[13] The Ma'adim Vallis head is among the most definitive indications that an overflowing paleolake carved the valley. Figure 1 illustrates the eastern valley and the large anastomosing tributary that enters from the southwest, both of which originate abruptly at gaps in the divide (degraded crater rim) separating the intermediate and Eridania basins. At the source for the eastern (main) valley, Ma'adim Vallis flows incised the drainage divide from its original ~1,200 m elevation and displaced the channel head 25 km southward to its present elevation of 950 m on the Eridania basin plains. The western gap is the source for the main valley's large tributary (Figure 4), which is discussed in more detail in section 3.4. Determining the initial elevation of the western gap is less straightforward, as a 28 km fresh crater formed adjacent to the gap after fluid flow had ceased in the tributary (Figure 4a). Fluidized ejecta from this crater partially filled the uppermost reach of the tributary valley and locally raised the elevation of the drainage divide. Modern topography suggests that the tributary source occurred at ~1320 m, but the precrater level can be calculated by subtracting the ejecta thickness δ, which thins with distance r from the center of a crater with radius R (in an ejecta blanket, $r > R$ meters). *McGetchin et al.* [1973] developed an ejecta thickness function for lunar craters:

$$\delta = 0.14R^{0.74}(r/R)^{-3}. \quad (1)$$

We estimate that the ejecta thickness declines to ~70 m at a distance of 34 km from the crater center, so that the original

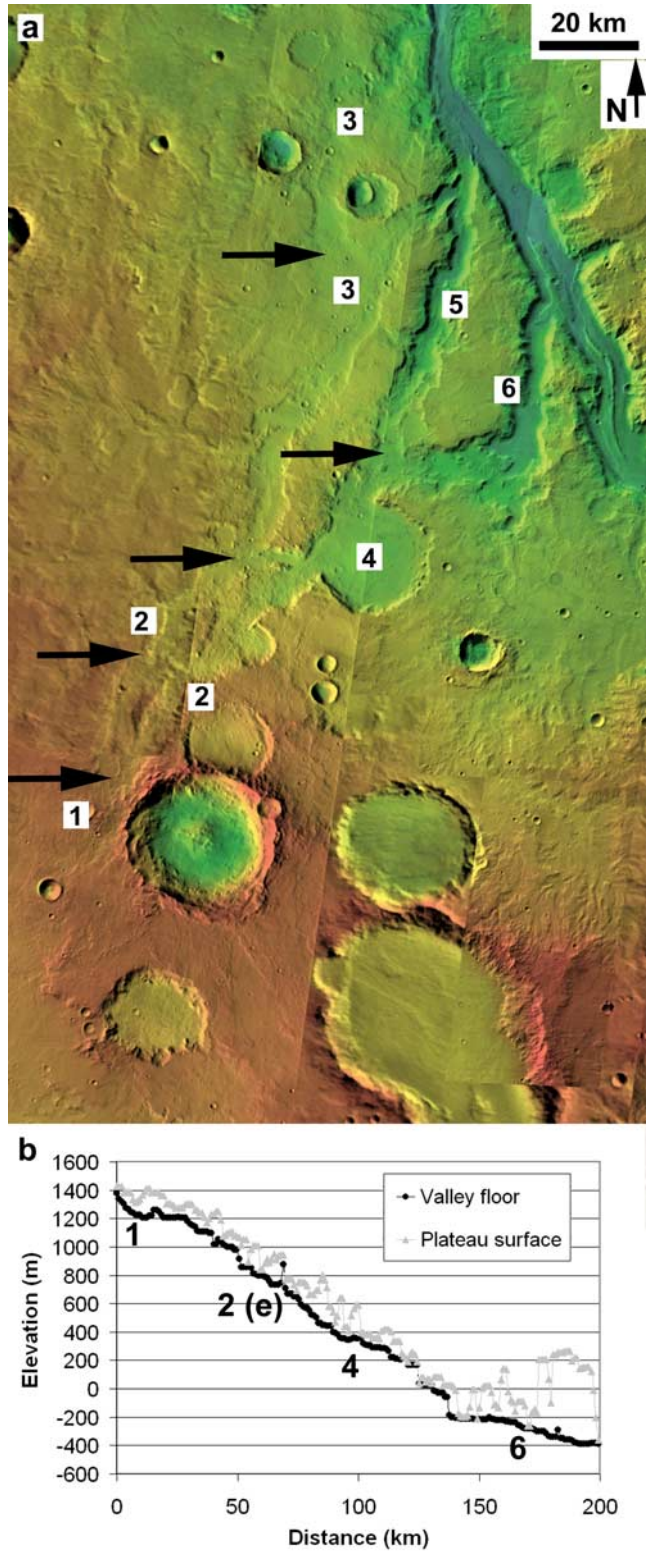

Figure 4. (a) The major tributary system to Ma'adim Vallis, with THEMIS daytime IR images overlaid on the Viking Orbiter Mars Digital Image Mosaic Version 2.1 and colorized with MOLA topography as in Figure 1. The valley originates at the intermediate basin drainage divide (1) and immediately divides into two anastomosing channels (2). Downslope bifurcations occur at sites marked by arrows. The western tributary courses (3) were abandoned early as a crater (4) captured the flows. Upon emerging from this crater, the flow again bifurcated along the intermediate basin floor to incise the deep tributary channels 5 and 6, which are graded to the Ma'adim Vallis floor. (b) Longitudinal profile of the easternmost flow path, which was the last to be utilized. The upper reach is incised only 100–200 m below the plateau surface (given as the highest point within 4 km of the channel thalweg), whereas the lower tributary reach was graded to the Ma'adim Vallis main channel floor, where it incised up to 600 m.

divide occurred at ~1250 m relative to the modern datum, close to the level of initial overflow of the eastern gap. This approximation is imprecise given that the crater occurs on Mars, where the gravity-controlled ballistic component of ejecta transport is shorter, but fluidized flows may extend the ejecta blanket.

[14] The morphology of the Ma'adim Vallis source points is consistent only with origin by paleolake overflow. Elevations in the Eridania basin decline to the south of the two valley heads, so no smaller valley networks could have supplied either of the Ma'adim Vallis source gaps directly, nor are such networks evident on the Eridania basin floor. *Malin and Edgett* [2000a] suggested that, in some areas, significant changes in topography occurred during the Noachian due to aeolian fill and removal. However, we find no constructive support in the geologic record (e.g., taller remnant mesas or pedestal craters) for ancient Eridania basin topography that would have allowed surface drainage to Ma'adim without ponding. Some aeolian deflation is evident in the Eridania basin, mainly of Electris air fall materials [*Grant and Schultz*, 1990] that appear to have been deposited after Ma'adim Vallis formed, as discussed below. Remnant mesas suggest that these sediments previously filled only a small portion of the total Eridania basin floor relief (Figure 5).

[15] Many valleys on Mars are attributed to sapping processes due to their poorly developed tributary networks and theater headwalls that may lack upslope tributaries [e.g., *Baker*, 1982; *Malin and Carr*, 1999; *Gulick*, 2001]. Whereas some terrestrial [*Howard et al.*, 1988; *O'Connor*, 1993] and Martian [*Irwin and Howard*, 2002] drainage divides appear to have been breached by headward migration of a sapping headwall, fed by surface water or groundwater on the opposite side of the divide, no headwall scarp occurs at the atypically wide Ma'adim Vallis heads, and no contributing aquifer (except the paleolake that we propose) occurred above the ridge crest where the valley source points occur. Furthermore, sapping without subsequent paleolake overflow is inconsistent with the discharges suggested by valley morphology, based on calculations presented In section 4.2. The western tributary developed an anastomosing course (Figure 4), which can occur when the topography cannot confine the volume of water it is required to deliver (as in the Channeled Scabland, Washington, U.S.A. [*Baker*, 1982, pp. 147–148]), or when aggradation of a channel floor forces the flow out of the channel [*Ritter et al.*, 1995, p. 221]. In this case, the large flow alternative is most reasonable, as no upstream surface was available to supply sediment to aggrade the floors of these large tributaries. The western paleolake outlet is more favorable to anastomosing channels relative to the eastern outlet, because fewer topographic obstructions were available to confine the western flow.

[16] Both the main and tributary channels are full-born, i.e., their ~3 km width at the source is similar to downstream channel dimensions. Sites of locally decreased channel width are associated with increases in slope as shown on the longitudinal profile (Figure 3) and remain consistent with a constant discharge in the down-valley direction. In contrast, Al-Qahira Vallis (Figure 6) is a valley network with a similarly wide lower reach, located ~400 km west of Ma'adim Vallis. Both valleys cross the dichotomy boundary and are incised a kilometer or more into cratered materials. Unlike Ma'adim, Al-Qahira Vallis originates through the confluence of narrow, ridge-bounded tributary networks. Ma'adim Vallis maintains its width even where it crosscuts impact craters, whereas crater breaches at Al-Qahira Vallis have variable width. The wide lower reach of Al-Qahira Vallis maintains a low, nearly constant gradient (Figure 6a), suggesting that the valley widened only after a stable base level was acquired.

[17] Although most Martian and terrestrial valleys originate immediately down-slope of their drainage divide, Ma'adim Vallis incised its initial headward divide to ~250 m depth, so that the present divide at the channel head is lower and projects 25 km southward into the Eridania basin. Headward displacement of the drainage divide is typical of terrestrial basin overflows. An analogous but much smaller catastrophic flood occurred on July 15, 1982, at Lawn Lake, Larimer County, Colorado, U.S.A. At this site, glacial scour of bedrock and development of a terminal moraine formed a natural basin of 66,370 m^2. An earthen dam was built on the moraine in 1903, artificially enlarging the precursor basin. Overflow of the composite dam stripped the unconsolidated dam and underlying glacial till down to bedrock, incising an outlet channel into the till and displacing the overflow spillway headward from its earlier position [*Jarrett and Costa*, 1986] (Figure 7). This overflow is particularly relevant to Mars. Before the flood, stream flows occurred on the surface of glacial till in the valley, as water may have flowed on the surface of similar Martian crater ejecta. With increased discharge during the Lawn Lake flood, a critical shear stress was reached to mobilize the bouldery glacial till, rapidly producing the modern deeply incised outlet valley. A much larger paleolake overflow could mobilize the Martian megaregolith similarly, as demonstrated in section 4.3, carving Ma'adim Vallis over a short time. A comparable but much larger natural dam failure occurred at Red Rock Pass, southern Idaho, U.S.A., on the northeastern margin of paleolake Bonneville

Figure 5. Morphology of positive-relief chaotic terrain and a remnant mesa of the Electris deposit in the deep crater subbasins. (a) The rough, high-albedo material that makes up the mesas is capped by a darker, more durable, thin cap rock (subset of MGS Mars Orbiter Camera (MOC) image M04-03292, centered at 35°S, 173°E). (b) MOLA track 14244, showing the positive relief of chaotic terrain relative to smooth plains on the depression floors. Dissected terrain occurs only above ~700 m, whereas lower-lying plains are smooth and undissected despite their steep slopes. Chaotic terrain is offset from the subbasin center. (c) MOLA track 16803, showing a remnant mesa of the Electris deposit overlying the Eridania basin floor plains. The Electris deposit did not fill the Eridania basin completely to the 950–1250 m elevations of the Ma'adim Vallis heads. The track also crosses two degraded impact craters with floor materials that slope toward the Eridania basin interior. (d) MOC Geodesy Campaign Mosaic for context. White line, 1100 m contour; black line, 700 m contour.

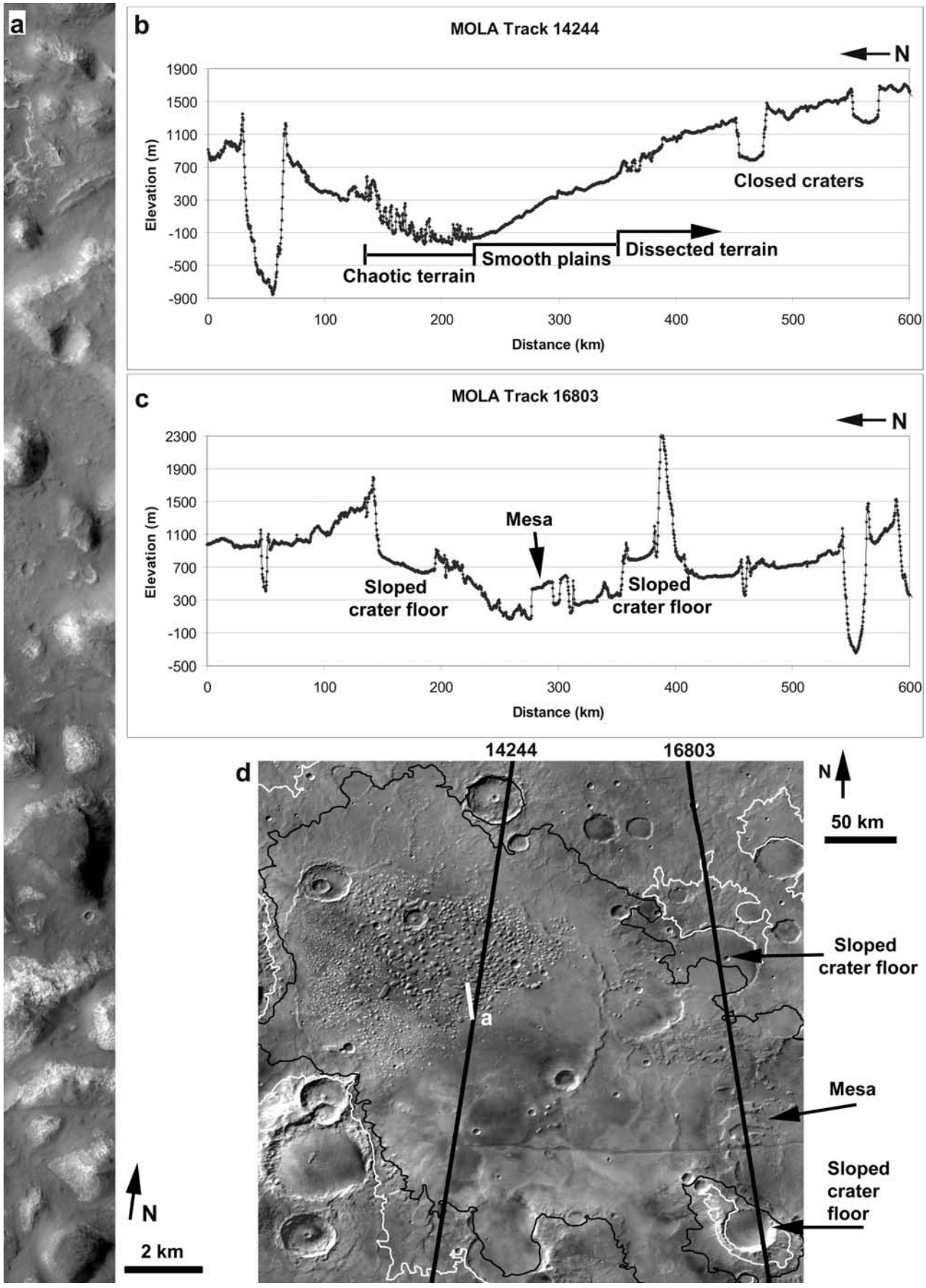
a
b
MOLA Track 14244
N
Elevation (m)
1900
1500
1100
700
300
-100
-500
-900
0
100
200
300
400
500
600
Distance (km)
Closed craters
Dissected terrain
Smooth plains
Chaotic terrain
c
MOLA Track 16803
N
2300
1900
1500
1100
700
300
-100
-500
Elevation (m)
Mesa
Sloped crater floor
Sloped crater floor
Distance (km)
d
14244
16803
N
50 km
Sloped crater floor
a
Mesa
Sloped crater floor
N
2 km

Figure 5

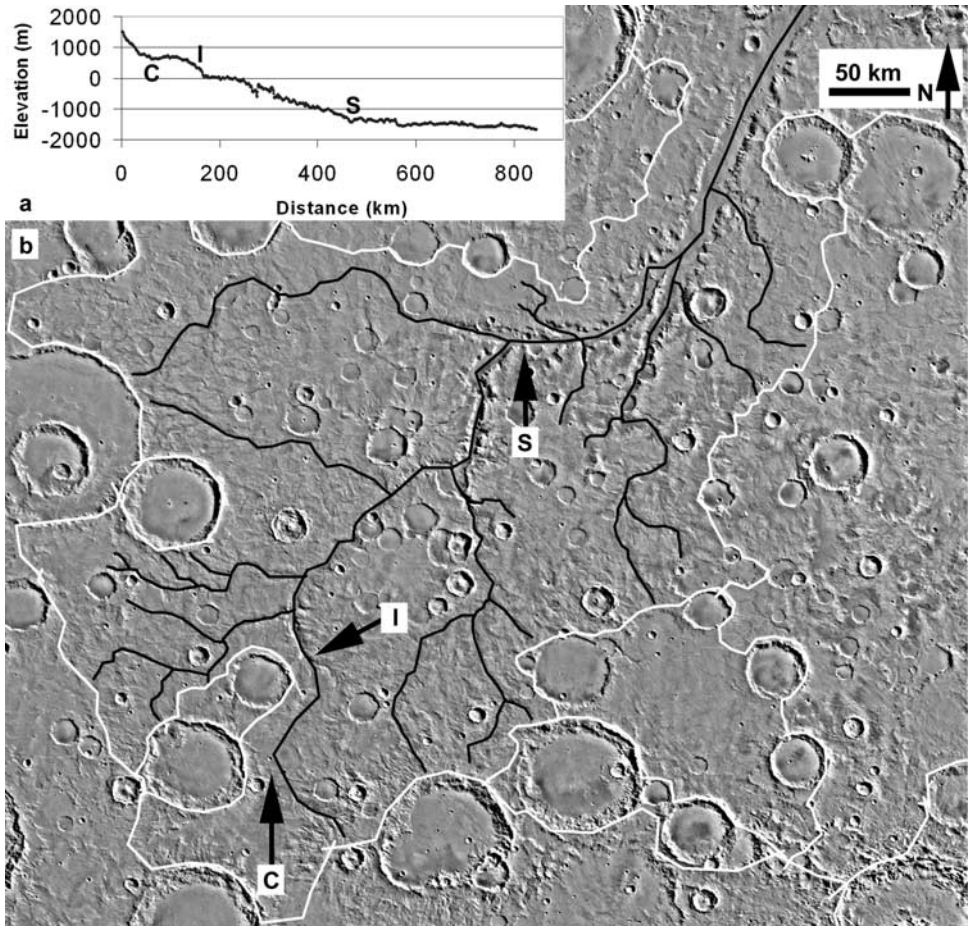

Figure 6. Al-Qahira Vallis. (a) Longitudinal profile of the main channel, which crosscuts a small crater (C) near the valley head. The valley is incised up to 700 m at I. The valley widens abruptly below S, where it acquires its base level at ~−1500 m. (b) Drainage basin of Al-Qahira Vallis, with major tributaries (black lines) and drainage divides (white lines) indicated. In contrast to Ma'adim, Al-Qahira Vallis grows from a space-filling tributary network rather than a large point source, and it is wide only in its lower reach.

about 14,500 years before present. The natural dam at this site was an alluvial fan, which impounded the lake at its highest (Bonneville) stage for several hundred years, yielding a lake of 51,530 km^2. The divide ultimately failed due to overtopping by the lake or headward growth of sapping channels (supplied by groundwater from the elevated lake) that developed in the unconsolidated fan material. A 108 m drop in lake level followed as the overflow channel stripped the fan down to bedrock, yielding a discharge of ~10^6 m^3/s [*O'Connor*, 1993]. Lake Bonneville experienced a rapid decline in level shortly after its single overflow, as the climate became progressively more arid [*Currey*, 1990].

2.2. High Internal Relief, Undissected Eridania Basin Impact Crater Floors

[18] The topography of the Eridania basin floor is atypical of basin plains in the Martian highlands, and characteristics of the floor topography suggested the occurrence of isolated paleolakes [*Howard*, 2000] before an association was made between a larger, integrated paleolake and Ma'adim Vallis [*Irwin et al.*, 2002]. Six highly degraded impact craters (180–240 km diameter) within the Eridania basin have atypically concave interiors, with high internal relief (up to 1 km) and relatively steep, inward-declining slopes (commonly 0.5–1.5°) (Figures 5 and 8). In contrast, most degraded impact craters >60 km in diameter on Mars have nearly flat floors, a sharp break in slope at the base of the crater wall, and decreasing floor relief with increasing crater diameter (Figure 9) [*Howard*, 2000; *Craddock and Howard*, 2002].

[19] Noncumulative hypsometric curves, or plots of the total area within elevation intervals, illustrate the concavity of these crater floors relative to normal Martian impact crater interiors at progressive states of degradation (Figure 9, Table 1). The depth of an impact crater usually declines with advanced degradation, as the rim is lowered and the interior fills. Hypsometric curves of typical Martian degraded craters peak at the lowest elevations (Figure 9), representing the large area of the nearly flat crater floors. This is contrary to the trend in the Eridania subbasins and in the nearby Newton and Copernicus craters, where the infilling material appears concentrated around the margins of the crater floors, so that the internal relief at the center was largely maintained. The high floor relief and morphology of these unusual crater floors can be recognized in the broad bench on the lower side

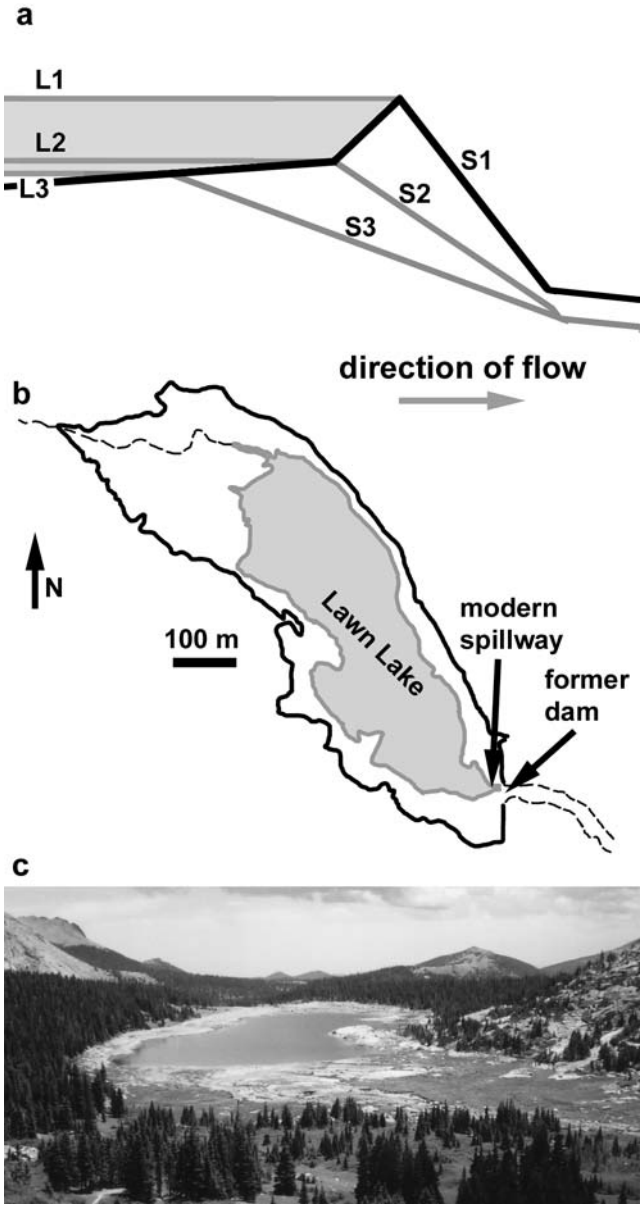

Figure 7. (a) Concept sketch of a paleolake overflow. The paleolake overtops the dividing ridge (black line) at the L1 level. Floodwaters downcut the divide with a relatively high stream power on the steep S1 slope, regrading the outlet to the lower S2 slope and releasing a large volume of water stored between the L1 and L2 levels. Further incision of the outlet below the L2 level suffers from lower slope and stream power, plus lower discharge released from the lake per unit of material that must be removed from the outlet valley. Ultimately, incision terminates and a remnant lake is impounded below the L3 level. (b) Lawn Lake, Colorado, showing the predamburst shoreline (black line) and the remnant lake (gray), adapted from *Jarrett and Costa* [1986]. Dashed lines show the inlet channel and the wide outlet channel carved during the flood. In this case, the incising channel encountered bedrock at the L2 level and no further incision was possible. The modern spillway occurs headward of the original dam crest as shown in Figure 7a. (c) The modern remnant lake and light-toned, exposed lake bed, facing down-valley to the southeast.

of the hypsometric curve (Figures 9h and 10). The Eridania basin hypsometry also differs from that of large fresh craters, which exhibit neither the bench nor a marked peak at the lower end of the curve (Figure 9e).

[20] The Eridania basin floor has been interpreted in part as volcanic plains [*De Hon*, 1977; *Howard*, 1979; *Scott and Tanaka*, 1986; *Greeley and Guest*, 1987], however the large relief within the plains is inconsistent with the flat or radially outward-sloping topography of more widely recognized volcanic landscapes on Mars (e.g., Solis, Lunae, or Hesperia Plana). Volcanic plains do not preserve concave depressions with deep central low points, as lava preferentially fills low areas in the topography. All degraded craters on the Eridania basin floor have concave floor deposits or floors that slope downward toward the center of the larger subbasin in which they are located (Figures 5c and 8). This contrasts with lava-embayed crater floors, which are typically flat or have a monotonic upward slope toward the breach through which lava entered the crater. As the Eridania basin craters are not embayed, the larger subbasins were not filled deeply or to a near-level surface, and no positive-relief volcanic constructs are evident in the area, volcanic resurfacing likely played a minor role, if any, in the present basin shape.

[21] The large relief of the Eridania basin floor suggests that the lower parts of the basin were shielded from fluvial erosion during the Noachian. As valley networks have formed on most >0.5° slopes in the region, it is likely that such valleys would have transported sedimentary materials toward the center of the Eridania basin over time, filling the depressions similarly to most other degraded craters [*Craddock et al.*, 1997; *Craddock and Howard*, 2002]. However, most of the large impact craters that form the subbasins have developed wide gaps in their original crater rims (Figure 8), so we must attribute some modification and infilling of the large craters to erosive processes rather than simple mantling. To collect the infilling material primarily around the margins of the craters, rather than in the center, sediment transport processes must have been relatively inefficient within the interiors of the large Eridania basin craters, consistent with the presence of standing water.

2.3. Absence of Valley Networks at Low Elevations

[22] Inhibited fluvial sediment transport within the deeper subbasins is consistent with the distribution of valley networks. In the deeper eastern subbasins, valley networks do not extend to the bottom of the lower-lying concave crater floors, despite the occurrence of regional slopes of 0.5–1.5° below 700 m elevation (Figures 5 and 11). Valley networks in the Eridania basin watershed terminate over a range of elevations, with most ending at the plains boundary between 1100 and 950 m (the elevation of the Ma'adim Vallis head). In localized, steeper sections of the Araidnes, Atlantis, and Gorgonum subbasin interiors, shallow valleys extend inward only to near the 700 m contour, whereas the low points of these subbasins occur at −200, −500, and −450 m, respectively. Dissection of steep slopes below 700 m occurs only in two localized areas, along the eastern margin of Ariadnes basin and the northern margin of Atlantis basin, where a few valley networks terminate at or above 300 m. In the eastern subbasins, valleys dissect the 1100 m contour along ∼90% of its length, but only ∼15% of the 700 m contour is crosscut, and no valleys extend below 300 m.

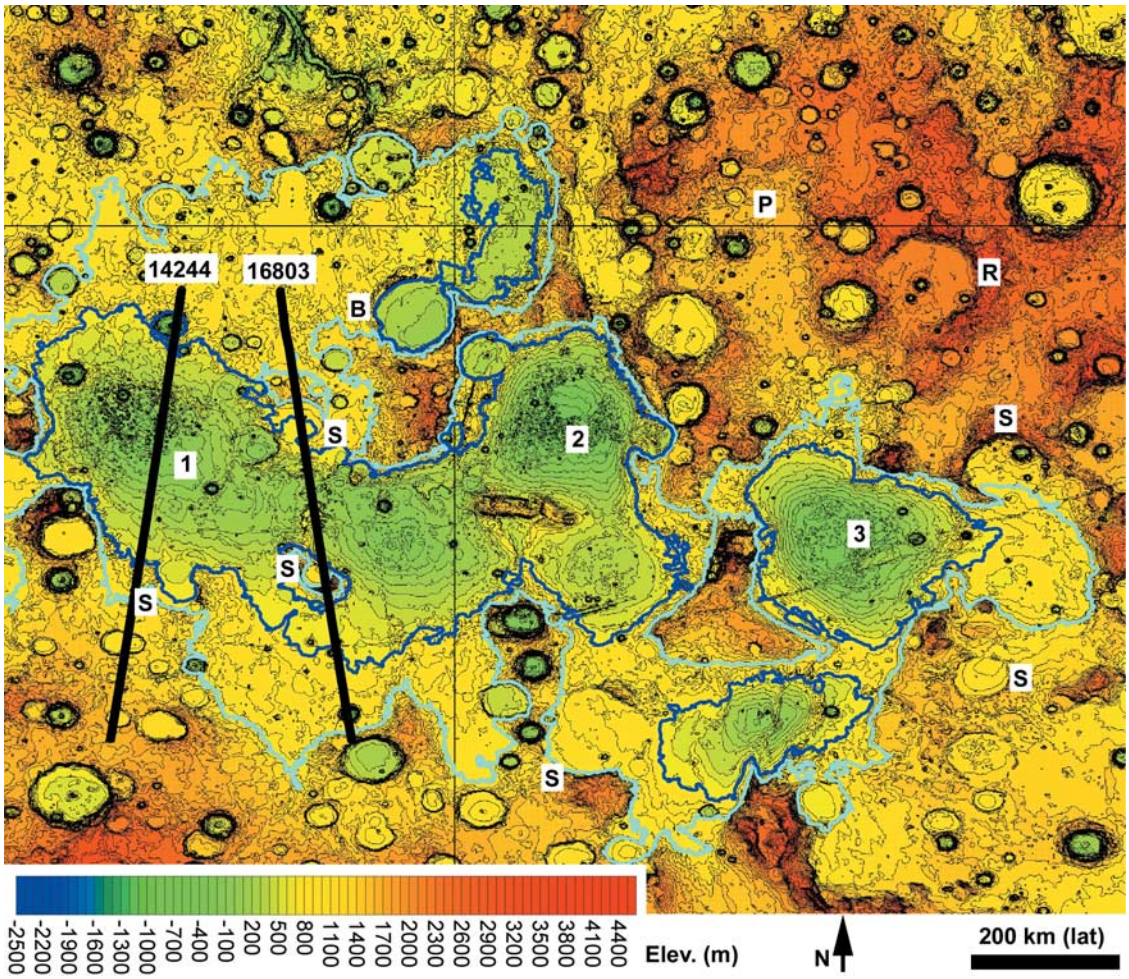

Figure 8. MOLA topography (60 pixels/degree, 100 m interval) of the eastern part of the Eridania basin. The MOLA tracks shown in Figure 5 are indicated. The large impact craters in this region maintained an unusually large floor relief and interior slope below 700 m elevation (dark blue line), relative to smaller degraded impact craters at higher elevations. The light blue line is the 1100 m contour, which is generally the plains/watershed boundary. One crater (B) has a wide breach in its rim. Some impact crater floors (S) above 700 m elevation slope downward toward the Eridania basin interior, demonstrating control of sediment transport by local slopes rather than a regional directionality as with aeolian deposition. These craters are not embayed by lavas from the basin interior, which is low-lying. Some impact crater interiors (R) have been reintegrated with surface drainage patterns, whereas other low-relief intercrater plains (P) were not integrated. Cratering generally created a multibasinal landscape. Named subbasins are indicated by (1) Araidnes, (2) Atlantis, and (3) Gorgonum.

Undissected relief within the Eridania basin floor therefore amounts to 500 to 1200 m depending on the subbasin. In the northwestern subbasin, no valleys were observed below 770 m. In high-resolution imaging, some rare, shallow, late-stage gullies dissect crater rims and other steep slopes across a wide range of elevations [*Malin and Edgett*, 2000b], but these gullies represent little geomorphic work.

[23] These observations suggest that fluvial erosion affected only the higher levels of the Eridania basin and that only spatially and temporally limited water sources were available to dissect topographic levels below ~700 m. In contrast, valley networks are common and extend to the drainage divides above 950 m. This pattern of elevation-controlled fluvial incision is consistent with the hypothesis that the deeper subbasins were occupied by standing water during much of the Late Noachian and Early Hesperian Epochs. Fresh impact crater walls and Sirenum Fossae graben provide a view of layered stratigraphy beneath the Eridania basin floor, where thin, blocky outcrops alternate with more friable layers (Figure 12). The more durable layers are resistant to aeolian erosion, and boulders are common in talus slopes at these sites. Layered deposits in the highlands are certainly not unique to a paleolake floor, but are consistent with the hypothesis. The thin, durable layers may have formed in response to cementation of sediments by precipitated minerals, although a definitive lithology cannot be determined with available data.

2.4. Indications of Former Lake Levels and Post-Noachian Adjustments

[24] Three types of landforms suggest a shoreline for the Ma'adim Vallis head paleolake, including (1) the overflow

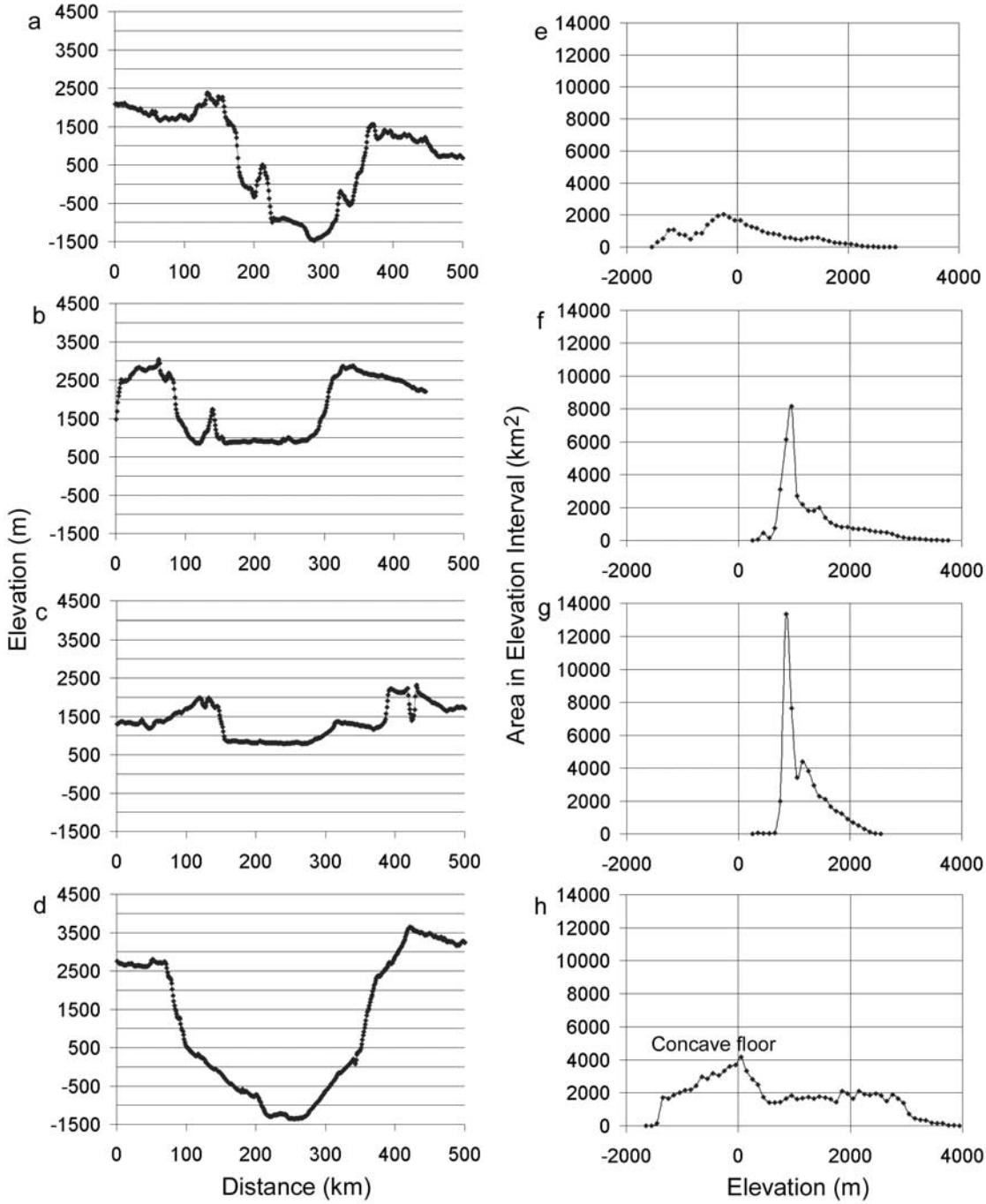

Figure 9. (a–d) Cross-sectional profiles of three peak-ring crater interiors at progressive states of degradation (Figures 9a–9c) compared to the interior of Newton crater (Figure 9d) without its exterior watershed. Newton is interpreted to have contained a separate paleolake. Most impact craters on Mars developed flat floors during degradation, so much of the floor area is concentrated within a narrow elevation interval. (a) Fresh Lowell crater. (b) Degraded Kepler crater. (c) Highly degraded Flaugergues crater, where the central peak ring has been largely removed or buried. (d) Newton crater, where infilling of the crater floor took place only around the margins of the floor, such that the original interior relief is largely preserved. (e–h) Noncumulative hypsometric curves (100 m elevation bins) of the degraded crater floors in (Figures 9a–9c), respectively, compared to Newton crater in Figure 9d. Newton exhibits a broad bench in the curve at lower elevations, instead of the usual peak in the curve at low elevations.

Table 1. Fresh and Degraded Impact Basins Used for Comparison With Eridania Basin Hypsometry

Crater	Location	Diameter, km
Lowell (fresh)	52°S 278.5°E	210 km
Kepler (degraded)	46.5°S 145°E	230 km
Flaugergues (degraded)	16.5°S 19°E	250 km
Newton (paleolake)	40°S 201°E	280 km

points, (2) the boundary of the Eridania basin interior plains, and (3) the termination of valley networks.

2.4.1. Overflow Points

[25] Two apparent overflow points occur on the Eridania basin divide, where the divide is breached to initiate Ma'adim Vallis. The western outlet occurred at ~1250 m and the eastern (main) outlet has been downcut from ~1200 m to 950 m. The original elevation of the eastern outlet is uncertain due to later incision, but it likely did not exceed 1200 m. Two other low points on the Eridania basin divide, at elevations of 1125 and 1170 m (points P1 and P2 on Figures 1 and 2, respectively), exhibit no evidence of overflow. These other low points require that the source paleolake level did not exceed 1125 m, if modern topography is an exact representation of its previous state [*Irwin et al.*, 2002]. However, the western outlet is 125 m and 80 m, respectively, higher than the elevation of the unused passes P1 and P2. Some postoverflow topographic movement is therefore necessary to account for the western tributary overflow. Here we examine candidate processes that have affected the Eridania basin topography.

[26] The P1 low point (elevation 1125 m) is only 200 km east of the eastern (main) Ma'adim Vallis source gap

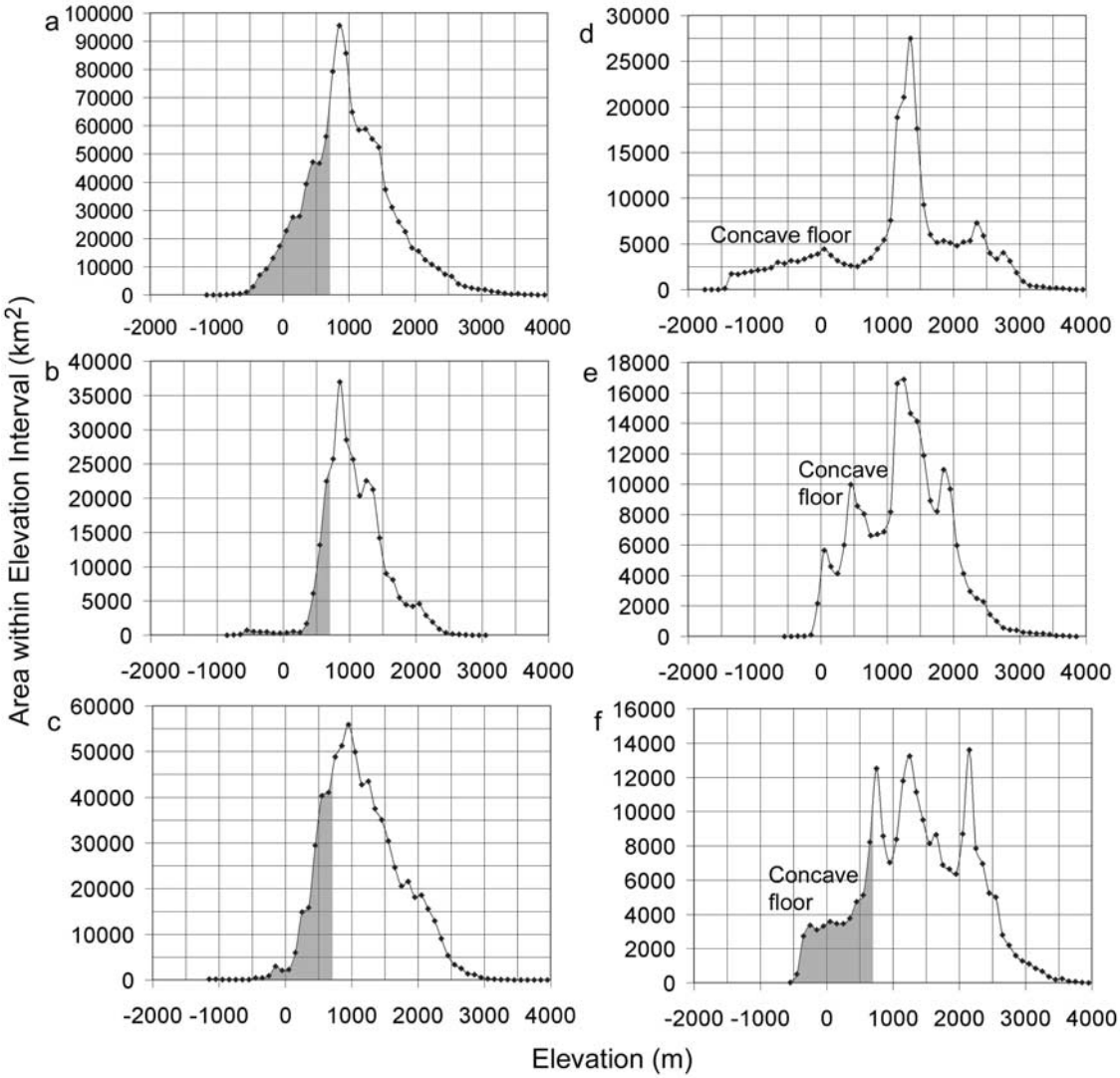

Figure 10. Noncumulative hypsometric curves (100 m elevation bins) of the Eridania subbasins and nearby Newton and Copernicus crater watersheds, as delimited in Figure 2. (a) Eastern subbasins. (b) Northwest subbasin. (c) Southwest subbasin. (d) Newton crater. (e) Copernicus crater. (f) Gorgonum crater and its watershed, which is one of the eastern subbasins. Curves are described in the text. The 700 m level is indicated in the Eridania basin, where valley networks commonly terminate despite steeper slopes below.

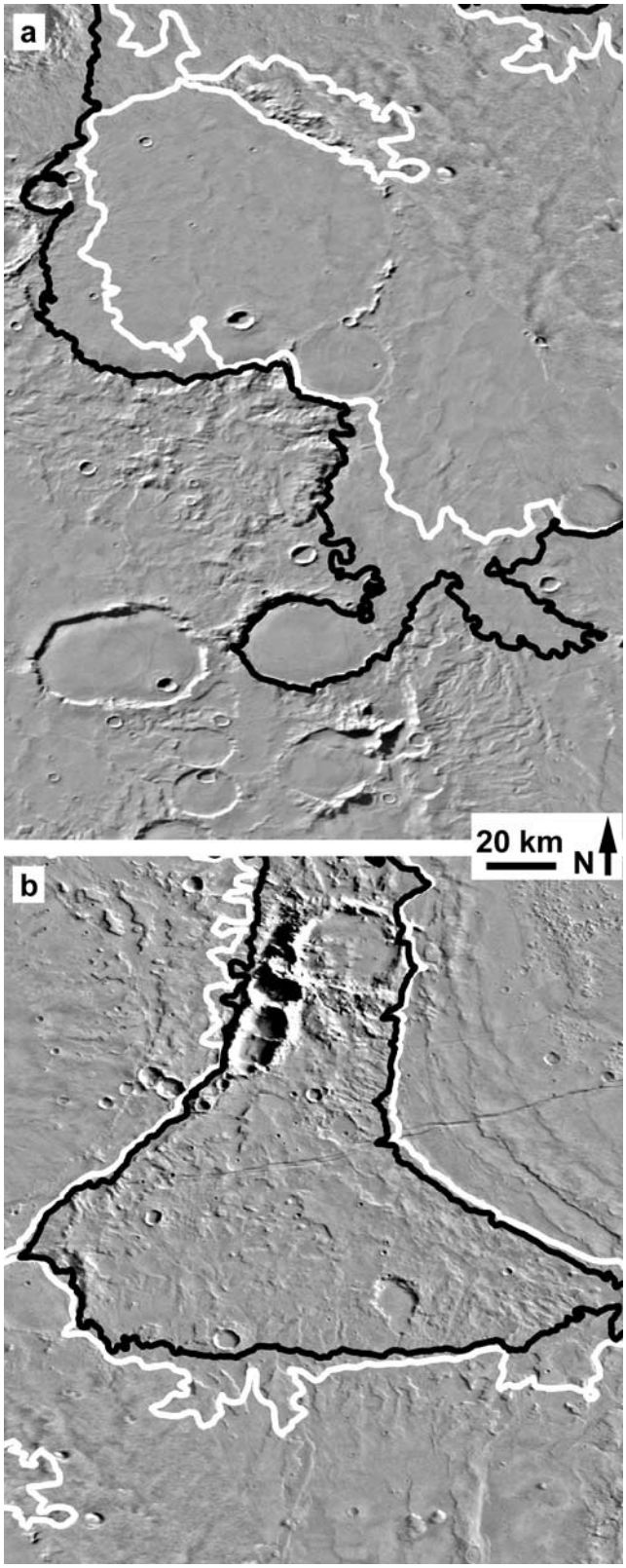

Figure 11. Valley network terminations in the Eridania basin shown in the Mars Digital Image Mosaic (MDIM) 2.1. Valley networks commonly terminate at the plains boundary between the 1100 m contour (black line) and the 950 m contour (white line), although valley networks locally extend down to the 700 m contour as in Figure 5d.

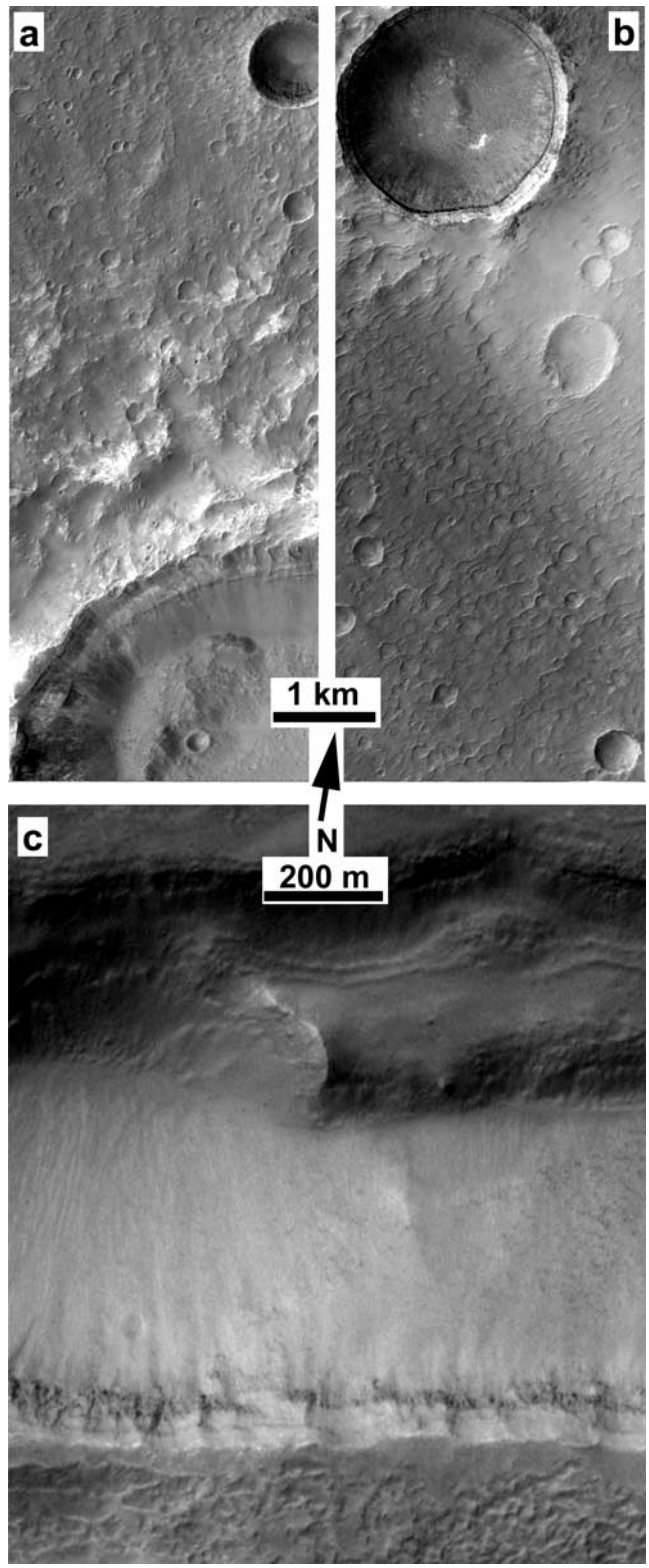

Figure 12. Layered stratigraphy in the Eridania basin floor. (a) Layering in a crater wall (MOC E11-00845, centered at 31.6°S, 193.6°W). (b) In another crater wall in the same image, layers are evident where high-albedo materials overlie a darker, thin layer. (c) High-albedo material overlying thin, dark layers in the Sirenum Fossae graben, which crosscut the Eridania basin floor (MOC M02-01583, centered at 38.9°S, 172.9°W, as shown in Figure 2).

(original elevation ~1200 m) (Figure 1). At P1, a 29 km, rimless degraded crater occupies the entire width of the pass. It is possible that during the outflow to Ma'adim Vallis, the rim of this crater still filled the pass, raising the present gap. On the basis of MOLA data analysis, *Garvin et al.* [2003] give the rim height h (m) for fresh complex craters of diameter D (m) as

$$h = 0.02D^{0.84}. \quad (2)$$

Assuming that the crater widened 10% with degradation [*Grant and Schultz*, 1993; *Craddock et al.*, 1997], a 26 km fresh crater would have a rim height of ~300 m, so this crater would provide the necessary blockage at a fresh or reduced state of degradation relative to its present form. As adequate fluvial erosion occurred after the main Ma'adim Vallis flow to incise its watershed tributary network, adequate time was available to erode this small crater to its present rimless form. Terrestrial bedrock erosion rates are typically highest on steep slopes, regardless of whether slope or fluvial processes are active [*Howard*, 1998], so ancient Martian crater interiors should have experienced high erosion rates relative to intercrater plains.

[27] To account for the 80 m discrepancy in elevation between the western source point and the P2 undissected pass, a westward tilt or declivity of 0.0001 (0.006°) would have to develop across the Eridania basin after the paleolake dissipated. Isostatic rebound may have influenced modern basin topography somewhat, but we have not modeled its effect. The eastern half of the Eridania basin contains Early Hesperian, Sirenum Fossae Tharsis-radial graben [*Anderson et al.*, 2001], and larger compressive ridges that are generally circumferential to Tharsis occur throughout the basin, so a growing Tharsis volcanic load may have adequately flexed the lithosphere after the overflow. *Phillips et al.* [2001] suggested that the Tharsis load (some of which must be post-Noachian to account for the young surface age) deformed the elastic lithosphere globally, but they did not specify the magnitude of the deflection. This load created uplifts at 80°E and 260°E, with corresponding topographic troughs centered at 170° (within the Eridania basin) and 350°E. The ridge of mountains located east of Newton crater (upper-right corner of Figure 2) may be a thrust belt of Late Noachian to Early Hesperian age, suggesting that crustal shortening and associated loading occurred in that area [*Schultz and Tanaka*, 1994]. By any of these means, a minor flexure of ~100 m amplitude could have been applied to the Eridania basin, accounting for the observed relationship between dissected O1 and O2 and the undissected P2 low point in the Eridania basin divide. At the present stage of understanding of Martian global geodynamics, we are unable to fully evaluate these possibilities.

2.4.2. Boundary of the Eridania Basin Interior Plains

[28] The boundary between the Eridania basin plains and higher dissected surfaces is displayed in noncumulative hypsometric curves in Figure 10. We delimited the watershed using MOLA topography (64 cells/degree), supported by the mapped extents of contributing valley networks. Peaks in the hypsometric curves correspond to low-gradient plains, which are elevation intervals containing relatively large areas. Within the Eridania basin, the subbasin curves exhibit three dominant features: (1) an exponentially decreasing area with increasing elevation above 1300–1400 m (typical of both eroded and cratered landscapes [*Grant and Fortezzo*, 2003]); (2) a break in slope below 1100–1200 m, transitioning to the Eridania basin floor plains that lie approximately between 700 and 1100 m; and (3) deep subbasins below 700 m in the east. The northwestern and southwestern subbasins have more level floor plains rather than deep depressions, so the lower ends of their hypsometric curves are steeper than is the curve is for all eastern (deeper) subbasins. The upper plains boundary in all of these subbasins is ~100 m below the elevation of the Ma'adim Vallis source gaps prior to incision of the valley, suggesting localization of sedimentary deposition below 1100 m. If flooding occurred to 1100–1250 m relative to present topography (the range of elevations incorporates possible later tilting), the entire Eridania basin would have contained a contiguous water body. The drainage basins of two large, concave floored, degraded craters adjacent to the Eridania basin, Newton and Copernicus, exhibit broad plains at higher elevations (1100–1400 m). The base level for erosion in these craters may have been somewhat higher than in the Eridania basin. Alternately, air fall deposits of 100–400 m thickness have also mantled these more southerly drainage basins [*Grant and Schultz*, 1990], raising the elevation of modern topography above the level of underlying plains.

2.4.3. Termination of Valley Networks

[29] As stated above, Hesperian valley networks that incise the Electris deposit do not continue into the deep subbasins within the Eridania basin, below about 700 m elevation. Other valley networks terminate at higher elevations where they encounter the Eridania basin plains (~1100 m) or other low-slope surfaces.

[30] On the basis of the hypsometric and morphologic evidence discussed above, we suggest that a paleolake occupied variable levels in the Eridania basin from ~700 to 1100–1250 m during the Late Noachian and Early Hesperian Epochs. During this time the paleolake inhibited fluvial erosion perpetually below 700 m elevation in the Eridania basin and occasionally at higher elevations. Sediments were generated from the degradation of topographic highs in the surrounding watershed, and these sediments were likely deposited and reworked within the Eridania basin as the water level rose and fell, over a long period or possibly in episodic or periodic cycles.

2.5. Discussion

[31] As liquid water does not occur on the Martian surface at present, identification of paleolakes must rely on related landforms or topography that remained preserved to the present time. Erosion rates declined in the equatorial Martian highlands after the Noachian [*Craddock and Maxwell*, 1993], so many features of that age are preserved, but ~3.7 billion years [*Hartmann and Neukum*, 2001] of post-Noachian processes now dominate the surface at meter to hectometer resolutions, or lower resolutions in some regions. Given that any Martian paleolakes probably had variable levels (as do terrestrial lakes) and must have ultimately dissipated with time, all levels of such water bodies were ultimately exposed to impact gardening [*Hartmann et al.*, 2001], aeolian processes, tectonism, and progressively limited fluvial and lacustrine processes.

Preservation of paleolake features therefore depends on large landforms relative to the thickness of younger deposits and the efficacy of more recent erosional processes. Shore landforms like bars, spits, and overwash are particularly susceptible to later erosion, or they may not form at all if a lake is perennially ice-covered [*French*, 1976, pp. 206–208]. Larger features and the morphology of Ma'adim Vallis provide the support for our inferences about the origin of the valley.

[32] As for all fluvial features on Mars, a debate continues over whether atmospheric or subsurface processes supplied the water. *Landheim* [1995] and *Cabrol et al.* [1997] proposed that Ma'adim Vallis was supplied by groundwater from Sirenum Fossae or from chaotic or knobby terrains, which occupy parts of the deep Eridania subbasin floors (Figure 5). However, the Hesperian graben [*Anderson et al.*, 2001] crosscut all other major geomorphic features in this area, and one smaller aligned graben crosscuts Ma'adim Vallis, so the timing does not support that hypothesis. Furthermore, the chaotic terrains lie ~1 km below and at least 370 km from the head of Ma'adim Vallis, so they could not supply water to the valley heads without first forming a lake. We also have no definitive indication that the chaotic terrain was a water source. The chaotic terrains do not occupy the full extents of their respective subbasins, and the groups of mesas are not always centered within the basins, so origin of the very deep basins by collapse is not suggested by the chaotic terrain morphology. It may be simply an in-place, eroded sedimentary deposit [*Lucchita*, 1982; *Grant and Schultz*, 1990; *Irwin et al.*, 2002; *Moore and Howard*, 2003].

[33] The second possibility is that precipitation supplied a source paleolake for Ma'adim Vallis. Fluvial erosion of the cratered highland landscape is indicated primarily by development of widespread branching valley networks that often head near sharp ridge crests (where groundwater sources are unlikely) [*Masursky et al.*, 1977; *Irwin and Howard*, 2002], locally basin-filling drainage networks [*Grant*, 2000; *Irwin and Howard*, 2002; *Hynek and Phillips*, 2003], degradation patterns of impact craters [*Craddock et al.*, 1997] and other basins [*Irwin and Howard*, 2002], ubiquitous loss of small Noachian craters (including on interfluves) [*Craddock and Maxwell*, 1990, 1993; *Strom et al.*, 1992], control of erosion by slopes on the order of ~1°, and the requirement for aquifer recharge to support sapping erosion [*Howard et al.*, 1988; *Goldspiel and Squyres*, 1991; *Grant*, 2000; *Gulick*, 2001]. For these reasons, the occurrence of a paleolake is consistent with other evidence for surface water summarized by *Craddock and Howard* [2002].

[34] Precipitation is the ultimate water source for perennial lakes on the Earth occurring above sea level, but these lakes are almost always connected with subsurface aquifers. Although a lake can initially form over a frozen layer in the substrate, a thermal gradient that is adequate to maintain the lake (including those with a seasonal or perennial ice cover) will ultimately provide heat to melt the underlying permafrost. In this case, the lake creates a connection to the groundwater system where one may not have existed beforehand [*French*, 1976, pp. 122–125], and the lake surface will ultimately respond to local hydraulic head as well as precipitation/evaporation controls. Alternately, if the climate is cold enough for the freezing front to extend below the lake floor, both the lake and subsurface will freeze. Salinity can impede wholesale freezing as a relatively fresh ice layer develops on the surface. In this manner, paleolakes in the Eridania basin may have maintained their connection with groundwater sources during less clement time periods. The Eridania basin crater depressions, and the similar concave floors of nearby Newton and Copernicus craters, are the lowest points on the Terra Cimmeria/Sirenum plateau. If an unconfined water table occurred anywhere within 1.5 km of the mean plateau surface (given frequent impact cratering, long-term confinement is unlikely), groundwater should have emerged in the deeper depressions.

[35] In this study, we are discussing a region in the midlatitudes, which would have been generally cooler than the equatorial regions except during periods of high obliquity [*Ward*, 1992]. The actual climate at the time and place of the Ma'adim Vallis outflow is uncertain, although annual temperatures near 0°C would minimize evaporation and help to maintain a paleolake on a relatively (to Earth) arid planet, particularly if it had a seasonal ice cover. Terrestrial lakes are most common in latitudes of 40–60° for this reason, relative to multibasin landscapes in warmer climates [*Cohen*, 2003]. It is also possible that melting polar ice helped to raise water tables over much of the highlands [*Clifford and Parker*, 2001], including in the Eridania basin. Basal melting of south polar ice sheets may have occurred over the same range of elevations that were occupied by the paleolake discussed here [*Head and Pratt*, 2001; *Carr*, 2002]. However, basal melting was not the only source for water, as many valley networks in the Eridania basin watershed and elsewhere originate at elevations of 2000–3000 m [*Carr*, 2002].

[36] We can only speculate on the cause of the Noachian/Hesperian boundary overflow as definitive indicators are not apparent. A period of greater water influx or reduced evaporation with a cooling climate may have allowed the level to rise. *O'Connor* [1993] suggests that groundwater sapping of alluvial fan material in southern Idaho initiated the Lake Bonneville flood, which then carved its own channel through a preexisting drainage basin. The sapping explanation seems unlikely in this case, however, owing to the contemporary development of two outlets. Two outlets are more reasonable for a large contributing head basin than for a small one. Unless the two outlets occurred initially at very similar elevations by chance, the lake would need to infill at a rate adequate to raise its level despite a small initial overflow discharge, activating the second overflow point. A large area or an abundant influx would make this possible. It is also possible that a small impact into the lake created a wave, which breached the Eridania basin divide more rapidly. A long-lived lake is expected to have sustained an impact flux comparable to outlying surfaces.

3. Basin Overflow and Development of Ma'adim Vallis

[37] The morphology of Ma'adim Vallis provides additional support for the overflow hypothesis. We begin with a discussion of the timing of the overflow, followed chronologically by controls on the valley course, influences on its cross-sectional and longitudinal profiles as it incised, and

the history of tributary development during and after the flood. We also calculate the flood discharge and briefly describe the deposits in Gusev crater.

3.1. Timing of Initial Overflow

[38] The timing of the paleolake overflow can be estimated using fresh crater counts on the Eridania basin, its watershed, and the watershed within the intermediate basin that supplied Ma'adim Vallis directly. Fresh craters overlie the widespread valley networks, so fresh crater counts provide a lower bound on the age of fluvial events [*Craddock and Maxwell*, 1990]. Several previous studies have produced variable crater counts for Ma'adim Vallis, which may reflect different data sources, crater diameters counted, or criteria for delimiting the valley [*Malin*, 1976; *Masursky et al.*, 1977, 1980; *Carr and Clow*, 1981; *Cabrol et al.*, 1998b]. Including the area between the top of the valley sidewalls, Ma'adim Vallis has 11 superposed fresh craters of >2 km in diameter, in an area of 15,100 km^2, but such small crater populations generate statistically insignificant age dates. In this study, we minimized the error inherent to small surface areas by dating the Ma'adim Vallis watershed's small tributaries (the contributing area within the intermediate basin and other small contributing watersheds) in addition to the trunk valley itself. The tributaries crosscut (are younger than) the trunk valley walls, so dating the tributaries maximizes the available area, minimizes the error, and allows both N(2) and N(5) counts to be used. The crater retention age, N(x) ± error, is the number of craters y greater than x km diameter in a specified area, $\pm\sqrt{y}$ error, with count and error normalized to an area of 10^6 km^2.

[39] Another apparent discrepancy is found in correlating crater counts of different diameter to the *Tanaka* [1986] stratigraphic scheme, whereby highland N(2) fresh crater counts can yield younger stratigraphic ages than N(5) counts from the same crater population. On this issue the reader may refer to discussion by *Tanaka* [1986] and *Hartmann and Neukum* [2001], and counts by *Grant and Schultz* [1990], *Tanaka* [1997], *Irwin and Howard* [2002], and *Irwin et al.* [2002]. The issue is that small crater counts on Tharsis lava flows, on which the stratigraphic scheme is based, apparently exhibit larger populations at <5 km than do highland units or the Vastitas Borealis Formation [*Tanaka*, 1986]. The discrepancy in small diameter populations may result from rapid degradation of small highland craters or a different population of impactors during heavy bombardment [*Barlow*, 1990], and more work is needed to define the scope and implications of the problem. Our N(2) fresh crater counts in this study area yield a late Hesperian age, whereas N(5) counts yield an age near the Noachian/Hesperian boundary on the stratigraphic scheme of *Tanaka* [1986] (Table 2, modified from *Irwin et al.* [2002]). *Cabrol et al.* [1998b] interpreted the young N(2) ages as indicating prolonged, episodic fluvial activity over 0.7 to 2.0 Ga in Ma'adim Vallis, starting in the Late Noachian Epoch and continuing throughout the Hesperian period. However, when the discrepancy in the highland crater data relative to the *Tanaka* [1986] scheme is recognized, the Gusev crater N(2) stratigraphic ages are actually consistent with the older ages suggested by larger-diameter highland fresh crater populations (Table 2), and the counts do not uniquely indicate a long period of activity. *Cabrol et al.* [1998b] and *Kuzmin et al.* [2000] also dated geologic units using crater counts on units with small surface areas. As shown in Table 2, the large errors inherent to such counts can result in widely variable stratigraphic ages, even when the discrepancy in the stratigraphic scheme is not considered.

[40] Regardless of which crater diameter is used to determine age, Table 2 shows that our N(2) crater counts on the Eridania basin floor are well within the error of the *Cabrol et al.* [1998b] results on Ma'adim Vallis and the Gusev crater floor. In Table 2 we have not included fresh crater populations for the southwestern subbasin, as pristine craters are rare south of ~40°S, where they have been more substantially degraded by recent air fall deposits or ice-related processes [*Jankowski and Squyres*, 1993]. Crater degradation and valley network activity appear to have declined at around the same time in the Eridania, intermediate, and Gusev basins, and the Eridania basin floor deposit and the Ma'adim Vallis tributary networks appear to be contemporary features (Tables 2 and 3). This timing is consistent with the regional decline in valley network activity and crater degradation that has been dated to near the N/H boundary using N(5) [*Maxwell and McGill*, 1988; *Craddock and Maxwell*, 1990; *Grant and Schultz*, 1990; *Irwin and Howard*, 2002]. With supporting evidence discussed below, the scenario of a long-lived Ma'adim Vallis can now be simplified by a brief flow near the N/H boundary (again using N(5) ages), with limited fluvial incision and resurfacing beyond that time.

[41] The longevity of the source paleolake is less certain. Whereas fresh craters provide a lower bound on its age, the only available upper bound is the middle Noachian age of the Npl_1 (cratered) unit in which the paleolake occurred [*Scott and Tanaka*, 1986; *Greeley and Guest*, 1987]. The

Table 2. Comparison of N(2) and N(5) Impact Crater Counts for Floors of the Eridania Basin, Ma'adim Vallis, and Gusev Crater

Geologic Unit	Count (y)	N(2)[a]	N(5)[b]
Eastern, NW subbasins <1100 m elevation	732	633 ± 27	192 ± 16
Gusev crater floor[c]	24	541 ± 221	none
Ma'adim Vallis floor[c]	5	708 ± 306	none
Ma'adim delta[c]	10	619 ± 206	none

[a]Absolute age interpretation from *Hartmann and Neukum* [2001]: Late Hesperian, ~2.9–3.6 Ga.

[b]Absolute age interpretation from *Hartmann and Neukum* [2001]: Late Noachian/Early Hesperian boundary, >3.5–3.7 Ga.

[c]Data from *Cabrol et al.* [1998b]. The large error in their results is due to small area of Gusev crater and small sample size.

Table 3. Fresh Crater Retention Ages for Hydrologic Units in the Ma'adim Vallis Region

Hydrologic Unit	Count (n)/Area, km^2	N(5)
Ma'adim watershed	41/208,500	197 ± 31
Main source subbasin (all)	199/1,089,000	183 ± 13
Main source subbasin watershed (>1,100 m)	83/463,300	179 ± 20
Main source subbasin floor (700–1,100 m)	66/363,500	182 ± 22
Main source subbasin floor (<700 m)	50/262,300	191 ± 30
NW source subbasin (all)	57/285,500	200 ± 26
NW source subbasin watershed (>1,100 m)	22/123,500	178 ± 38
NW source subbasin floor (<1,100 m)	35/162,000	216 ± 37

paleolake was therefore present during a fraction of the ~250 Ma included in the Middle and Late Noachian Epochs [*Hartmann and Neukum*, 2001]. At a minimum, the lake was present from near the time of formation of the larger, deep subbasins, which were not extensively modified below the 700 m level by fluvial sediment transport or valley incision. Fresh crater retention ages at different levels of the Eridania basin floor are similar to those of the higher-standing watershed and the dissected intermediate basin (Table 3), so the larger source paleolake did not persist for long after the valley network activity ended in the Ma'adim Vallis watershed. Some water may have collected in the Eridania basin depressions episodically into the late Hesperian [*Howard and Moore*, 2004].

3.2. Development of Flow Path

[42] We tested the overflow hypothesis by reconstructing the topography of the Ma'adim Vallis region prior to incision of the valley, to determine whether overland flow would pursue the present course given point sources at the valley heads. Given that Ma'adim Vallis typically has a sharp break in slope at the top of the valley sidewalls, and only minimal erosion appears to have occurred after the flow, the valley remains sharply defined, and backfilling produces a close approximation of the antecedent surface. We deleted the valley from the 64 pixel/degree MOLA digital elevation model (DEM) and refilled the DEM by kriging (Figure 13). The volume added to fill the valley in this process, ~14,000 km^3, closely matches independent estimates of the valley's volume calculated from individual cross sections [*Goldspiel and Squyres*, 1991; *Cabrol et al.*, 1996; *Irwin et al.*, 2002]. The reconstruction is therefore generally accurate, but it is not precise at all points, as some grid cells are filled somewhat too little or too much by this method.

[43] The Ma'adim Vallis course favors the overflow hypothesis. The reconstruction of prevalley topography shows that antecedent topographic gaps and impact craters would have controlled overland flow (arrows in Figure 13), producing the modern sinuous valley course exactly as shown in Figure 1. Water originating from the outlets (points A in Figure 13) was directed into the intermediate basin by the topography of several impact craters and other preexisting drainage divides (points B–E) near the intermediate basin rim. Water overflowed the northern intermediate basin divide (point F) and was channeled toward Gusev crater by two ridges (points G and H) that lie perpendicular to the dichotomy boundary. Along this lower reach, the Ma'adim flow exploited an older drainage basin, similar to those occurring to the east and west along the dichotomy boundary slope (Figure 1). The ridges delimiting this old drainage basin (G and H) directed water across the lower-standing, eroded rim of overlapping New Plymouth and Downe craters (C1), which are superposed on the Gusev rim. Down-cutting along this topographically controlled course created the entrance breach to Gusev crater.

[44] Impact crater rims appear to have resisted erosion more than did other landforms. The flow crosscut five impact craters (Figure 13, points X, C1, and C2) only where other ridges, standing higher than the previously eroded crater rims, directed flows through a crater. Otherwise, the rims of impact craters as small as 17 km diameter diverted the valley course around the crater. This control of the valley course by prevalley topography (without exception) invokes overland flow of water rather than headward erosion by structurally controlled groundwater sapping.

[45] A tectonic origin of the valley [*Brakenridge*, 1990] is considered unlikely on the basis of the following observations: (1) Ma'adim Vallis is a sinuous valley rather than a linear feature, it changes its longitudinal direction liberally, and the valley is comparably wide in its north-south, east-west, and intermediate orientations. (2) Extension related to an east-west principal stress is not evident in other landforms in the area, and no observed extensional faults radiate from the head, terminus, or bends of Ma'adim Vallis (mapping by *Brakenridge* [1990] shows this lack of graben with appropriate orientations). While the lack of observations does not preclude the existence of appropriate extensional fault structures, we are unable to validate a tectonic contribution to the valley. (3) Some impact crater rims are breached, but the rims are not displaced to widen the crater in the cross-valley direction. A "left-laterally displaced" crater discussed by *Brakenridge* [1990] is actually two overlapping craters that have been collectively breached [*Landheim*, 1995; *Milam et al.*, 2003]; generally, very little evidence of strike-slip motion on Mars has been observed. (4) Valley bends are curved as would be expected for a wide flow, not intersecting lineations as would be expected for a structural valley. (5) We have demonstrated that the course of the valley is entirely consistent with control by prevalley topography. A tectonic hypothesis fails at this time for a lack of constructive support, in addition to inconsistencies with observations given here. These observations are also inconsistent with structural control of groundwater flow [*Brakenridge*, 1990]. Aeolian and volcanic hypotheses for the origin of Martian valley networks and outflow channels have been discussed in depth and refuted in earlier literature [e.g., *Carr*, 1974; *Baker*, 1982], so such a discussion need not be repeated here. The paleolake overflow concept, in contrast, offers an internally consistent story that explains the observations well.

3.3. Incision of the Ma'adim Vallis Lower Reach

[46] Overland flows from the Eridania basin were initially impounded in the adjacent intermediate basin (Figures 1 and 13). The intermediate basin's overflow point at 1000 m (on its northern side) suggests a basin volume of ~60,000 km^3, of which <10% is the eroded volume of the upper and intermediate reaches of Ma'adim Vallis. The intermediate basin may have filled slowly prior to the Eridania basin overflow, by atmospheric sources and/or northward seepage

Figure 13. (a) Reconstruction of topography prior to the Ma'adim Vallis outflow, from the 32 pixel/degree MOLA grid. Arrows indicate the flow paths, where preexisting ridges and craters channeled overland flow from the Eridania basin. Sites are described in the text. (b) The lower reach of Ma'adim Vallis, from the knickpoint through the Gusev exit breach. THEMIS daytime infrared mosaic overlaid on the Viking Orbiter MDIM 2.1 and colorized as in Figure 13a with MOLA topography.

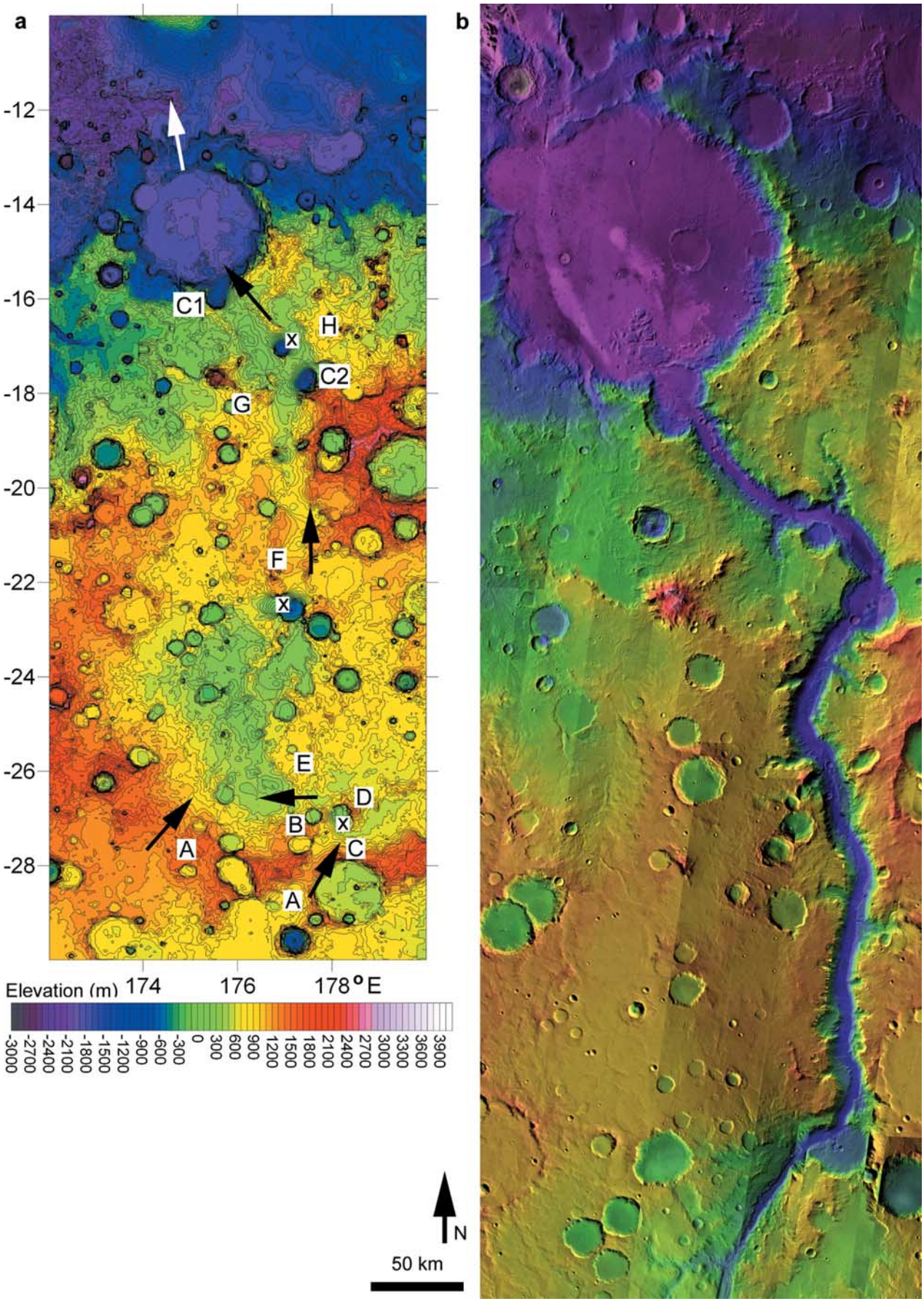
a
b
-12
-14
-16
-18
-20
-22
-24
-26
-28
C1
H
C2
G
F
E
D
B
C
A
A
Elevation (m)
-3000 -2700 -2400 -2100 -1800 -1500 -1200 -900 -600 -300 0 300 600 900 1200 1500 1800 2100 2400 2700 3000 3300 3600 3900
174
176
178°E
N
50 km

Figure 13

of groundwater, or overland flow from the Eridania basin may have filled it rapidly. As we discuss below, constrained estimates of the total volume discharged would allow either of these scenarios. Being initially covered with standing water, the floor of the intermediate basin could not be eroded until the lower reach of Ma'adim Vallis (north of the intermediate basin) was incised, allowing the basin to drain.

[47] Inward-sloping terraces along the wide lower reach of Ma'adim Vallis, from the intermediate basin exit breach to Gusev crater (Figure 14), may represent a wider channel floor that was active during a peak discharge from the intermediate basin. The terraces are likely not resistant outcrops, as they do not constrict the channel relative to its width in the intermediate reach, and they do not affect the longitudinal profile. Including the width of the terraces, the lower reach's valley floor is wider (~9 km) than are the floors of the intermediate and upper reaches (~5 km), although the lower reach's inner channel has a similar width of ~5 km. Given that the lower reach was incised first, its width may reflect earlier flow conditions. Channel width increases with the square root of discharge [*Knighton*, 1998]. Filling the intermediate basin to its overflow point (~1000 m) would not impede further influxes from the Eridania basin, where water stood at a higher level (originally 1100 to 1250 m). Therefore, as the northern divide of the intermediate basin was incised, water would be released from storage in the intermediate basin, while water would simultaneously flow from the Eridania basin into the intermediate basin, temporarily increasing the total discharge, erosive power, and width of the Ma'adim Vallis lower reach.

[48] Another important influence on paleolake discharge would be the incision rate at the valley head gaps. For an Eridania basin paleolake of $\sim 1.1 \times 10^6$ km^2 (the area below the 1100 m contour) some $\sim 10^4$ km^3 of water would be available for discharge per each 10 meters of outlet incision. If the outlet incision was initially more rapid than the decline of the Eridania basin's water level (e.g., if surface materials were poorly consolidated relative to underlying bedrock), the discharge would increase for some time, and a peak flood would occur. Increasing resistance of deeper, better-consolidated materials would then retard the incision rate, and the paleolake's water level could decline, reducing the flow depth and discharge. The lower reach terraces occupy a lower level (−300 to −700 m) than the intermediate basin floor (+400 m), so the high discharge from the Eridania basin probably outlived the peak discharge from the intermediate basin.

3.4. Development of Western Anastomosing Tributary

[49] The simultaneous activity of two overflow points, the Ma'adim Vallis main channel and its large anastomosing tributary, contributed to the peak discharge, but more rapid incision of the eastern outlet ultimately left the western outlet abandoned above the falling lake surface. The large western tributary originated at the western gap in the Eridania basin rim (Figure 1, point O2; Figure 4, point 1). This western overflow immediately divided into two anastomosing channels near the ridge crest (Figure 4, points 2), which suggests that the sloping topography at this site was unable to confine a large flow. Tributary flows initially ran out onto the intermediate basin floor, incising the westernmost paleochannels (points 3), and the water also overtopped the rim of a degraded 21 km impact crater on the intermediate basin floor (point 4). This crater captured the tributary flow, so that the westernmost tributary course was abandoned early. Upon exiting this small crater, unconfined water again flowed across the intermediate basin floor toward the site of the main Ma'adim channel flows, and

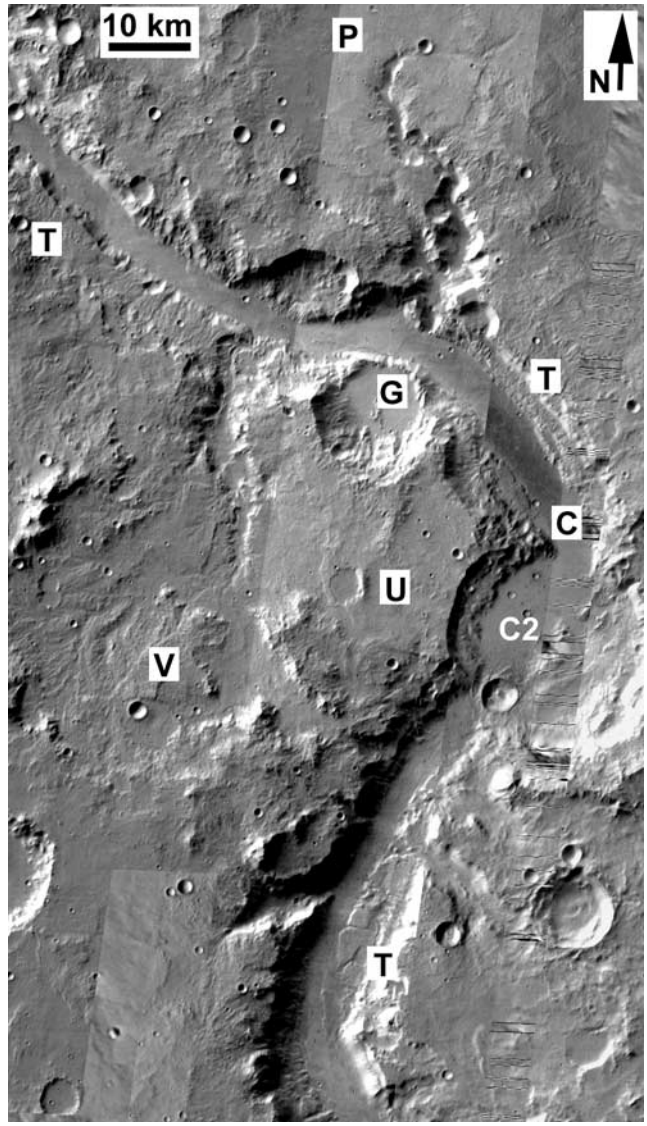

Figure 14. Terraces (T) and erosion of the lower reach of Ma'adim Vallis in THEMIS daytime IR imaging. The rim of the crater G was eroded during the terrace-level flooding and then the rim remnant confined the flow as the valley incised its present inner channel. Gullies dissect the terraces and valley walls, and space-filling valley networks (V) dissect sloping terrain in the watershed. Plains surfaces (P) are poorly dissected, but they collected water to incise stem valleys headward. Flat areas remained undissected (U). The crater C2 is rimless, which allowed the crater to be breached widely by the inner channel (C). The former C2 rim did not divert flows around the crater, as nearby low-lying ground at U is undisturbed.

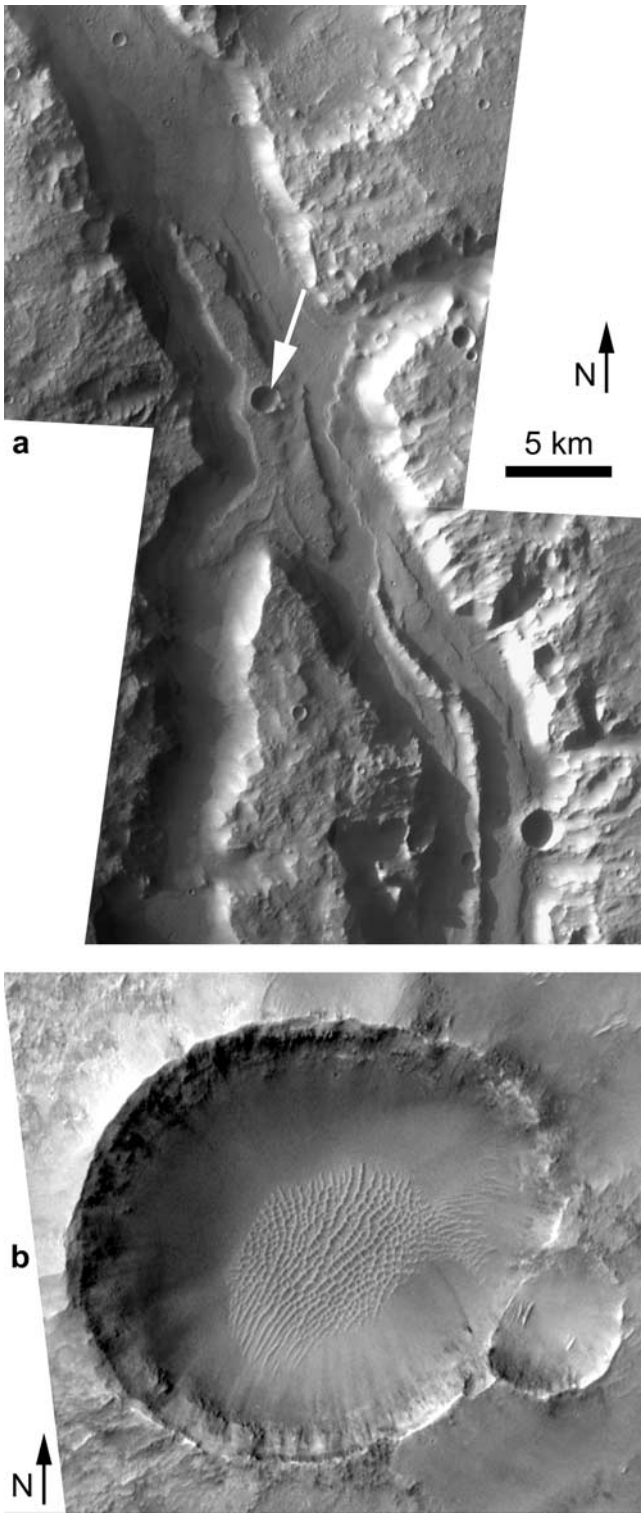

Figure 15. (a) Medial bar at the confluence of the main valley and western tributary in mosaic of THEMIS V05612003 and V05250002. The bar is 1–2 km wide and stands 120 m above the floor of the valley, which is ~700 m deep at this location. (b) At the white arrow in Figure 15a, a 1.4 km impact crater excavated part of the bar, exposing visible layers at the 3.5 m resolution of MOC image E05-01177.

two lower tributary reaches were incised (points 5 and 6). As these reaches down-cut and advanced headward, they confined the flows crosscutting the 21 km crater. The eastern lower tributary reach (point 6) crosscuts the western lower reaches (points 3 and 5), suggesting that the eastern reach ultimately captured the entire flow. Layered bar deposits (Figure 15) are preserved mainly at the confluence of this easternmost tributary reach and the main valley, supporting its relatively late activity. In this manner, one source point fed anastomosing tributary channels with three outlets into Ma'adim Vallis.

[50] As the larger tributary valleys are graded to the present floor of the main channel at −400 m elevation, the Ma'adim lower and intermediate reaches must have incised to this level either before the tributary flow occurred, or contemporary with the tributary development. Furthermore, a depositional bar and a streamlined ridge on the main channel floor appear to have been influenced by large flows from both the main channel and eastern distributary simultaneously (Figure 15). These observations support the overland flow sequence whereby the lower reach of Ma'adim was incised first, draining water from the intermediate basin and then allowing the upper reach of the main channel and its broad western tributary to incise. At this point, tributary flow declined and the western overflow point was abandoned. The other possibility is that the western tributary flow initiated after the eastern outlet discharge had already done most of the work, but this scenario requires a rapidly increasing Eridania paleolake level during the overflow flood and/or some means (e.g., ice) of temporarily damming the eastern outlet. The added complexity of such a scenario does not seem required by observations, but it cannot be ruled out at present.

3.5. Late-Stage Incision

[51] The final stage of Ma'adim Vallis incision involved only water from the eastern source point (O1 in Figure 1), which cut the upper reach of the main valley ~300 m below the upper reaches of the western tributary. This late stage also incised and regraded the lower reach to a −1550 m terminus at Gusev crater. As is typical of craters emplaced on a regional slope (the dichotomy boundary), the southern rim of Gusev crater was higher than its northern, downslope rim, which stood at <−1250 m elevation prior to the flood. A Gusev crater paleolake, supplied by Ma'adim Vallis, could only provide base level control once the lower reach of Ma'adim Vallis (including the entrance breach of Gusev crater), had incised to −1250 m. Exit breaching of Gusev crater was required prior to the final ~300 m of base level decline and incision of the Ma'adim Vallis inner channel. The modern exit breach on the northwestern side of Gusev is incised to −1550 m, which corresponds with the −1550 m level of the putative Gusev delta [*Schneeberger*, 1989; *Grin and Cabrol*, 1997]. The −1550 m base level at Gusev and a postpeak discharge were active as the wide inner channel was graded to its nearly constant slope of 0.0012 (Figure 3).

3.6. Alternative Histories

[52] *Cabrol et al.* [1996] proposed a sequence of events for Ma'adim Vallis involving a long-lived valley and multiple disruptions by impacts. In their model, Ma'adim Vallis

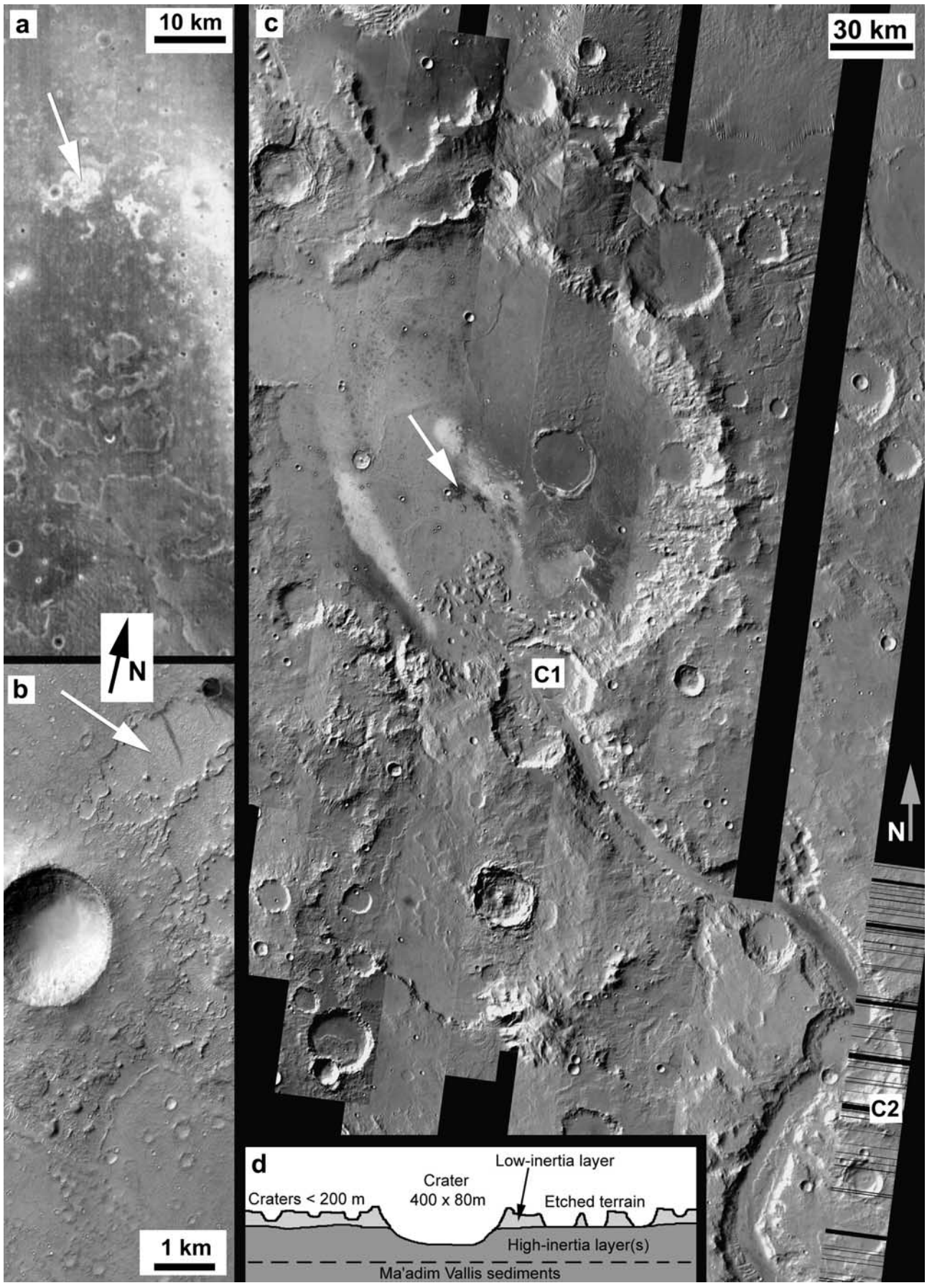
a
10 km
b
N
1 km
c
30 km
C1
N
C2
d
Low-inertia layer
Crater
400 x 80m
Craters < 200 m
Etched terrain
High-inertia layer(s)
Ma'adim Vallis sediments

Figure 16

first debouched to Gusev crater along its western rampart before entering Gusev at the present entrance breach. Present topography show that this scenario is not possible, as no breach occurs through the confining ridge G in Figure 13b. After the valley was incised, they suggest that two 30 km craters (C1 and C2 in Figures 13 and 16) interrupted Ma'adim Vallis, creating temporary intravalley lakes. Given the detailed imaging and topography that is now available, we find no evidence that these craters are younger than Ma'adim Vallis. In the case of crater C1 (Downe/New Plymouth), the higher preexisting ridges G and H in Figure 13 would simply direct water across the C1 crater rim and into Gusev, so there is no need for a putative disrupted Ma'adim Vallis to deliver water to breach this crater rim. In the case of the crater C2, its rim (in a fresh state) would have redirected flow through a broad low point to the west of the crater (near U in Figure 14), but the site is undissected. As flows in fact crosscut the crater rather than diverting to the west, the C2 crater rim must have already been eroded when overland flow reached this site. The modern C2 crater profile is rimless (Figure 14). *Cabrol et al.* [1996] used radar data to determine the valley's longitudinal profile, which appeared to have a reverse slope along part of its length. They attributed this reverse slope to sedimentation near the crater dam. In MOLA data, this anomaly does not occur (Figure 3), and sedimentation initially occurs primarily at the head of a lake, not near its dam. For these reasons and given consistent crater counts, we find no compelling evidence that Ma'adim Vallis evolved over a long period, with interruptions as described in earlier papers. The relationship between the valley course and other topography, including breached impact craters, is entirely consistent with brief development during an overland flood.

3.7. Gusev Crater Deposits

[53] Thorough descriptions of the Gusev crater floor morphology have been prepared for the MER mission, detailing the physiographic units [*Kuzmin et al.*, 2000; *Milam et al.*, 2003] and features related to the crater's wind regime [*Greeley et al.*, 2003]. We therefore limit our discussion to the floor stratigraphy. The exposed floor materials contain at least two major layers, which are evident from high-resolution visible and infrared imaging (Figure 16). The upper layer is discontinuous and has a variable thickness up to tens of meters. Wind has recently stripped this apparently friable unit in some places to form etched terrain, with enclosed depressions some tens of meters deep, and at other locations it may have been removed completely. In etched terrains, the surface layer appears to have a more resistant cap, which favors degradation by scarp backwasting prior to deflation of the material. The thin surficial layer may be a lacustrine, ash, or other air fall deposit.

[54] Removal of this layer and gardening by craters of >200 m diameter has exposed a deeper layer with higher thermal inertia (Figure 16). The gardened material has capped the friable material to form a partial pedestal crater at one site (Figure 16b). This underlying layer is thick enough to make a significant contribution to crater ejecta, but it is too coarse to be deflated significantly by wind. This deeper material may be a coarse deposit from Ma'adim Vallis, a layer of basalt, or one material overlying the other as shown in Figure 16d. Early results from the Spirit rover suggest basalt at the surface [*Grant et al.*, 2004], which may locally overlie the friable layer, or the friable material may be stripped at the landing site to expose underlying basalt. These hypotheses were considered among others at the landing site selection meetings before the MER launch, as the Apollinaris Patera volcano is located immediately to the north of Gusev. Regardless of the nature of the surface layer, the volume of sediment deposited in Gusev crater ($\sim$15,100 km^3 [*Carter et al.*, 2001]) closely matches the volume eroded from Ma'adim Vallis ($\sim$14,000 km^3), so fluvial sediments may comprise the greater part of the Gusev fill material. Gusev likely acted as a terminal basin or a runoff detention and settling pond for any flows that entered the crater [*Schneeberger*, 1989; *Grin and Cabrol*, 1997].

4. Flood Magnitude

4.1. Total Volume Discharged

[55] The Eridania basin overflow can be characterized by the total volume of the flood and by the dominant discharge that was responsible for the valley geometry. Although the Eridania basin topography might allow a straightforward calculation of total overflow volume, tectonic activity, air fall deposits, and aeolian deflation (discussed below) have modified the basin after the flood, and a precise indication of the former shoreline (our estimate is $\sim$1100–1250 m as discussed above) is not available given subsequent resurfacing. Here we bracket the total discharge that would be available from a single overflow of the Eridania basin to test the hypothesis that the valley could be carved in a single flood, although multiple overflows may have occurred. These results offer greater precision than those presented by *Irwin et al.* [2002], and we now incorporate a revised estimate of lake levels associated with the western anastomosing tributary.

[56] For a conservative estimate of the total volume discharged from the Eridania basin, we assume that the

Figure 16. The lower reach of Ma'adim Vallis and Gusev crater. (a) THEMIS night IR image I01511006, showing patches of coarse (thermally bright) materials in the ejecta of craters superposed on the Gusev floor. Patches of coarse material are also exposed to the east of an impact crater (white arrow). (b) These exposures of coarse material correspond to the low areas within etched terrain, where a superjacent layer tens of meters thick has been stripped by wind (white arrow; MOC image E17-00827). (c) Context of Gusev crater in daytime infrared, showing the location of thermally dark etched terrain shown in Figures 16a and 16b (white arrow). This coarse material is also exposed in a broad area in the southeast part of the crater, again corresponding to the location of etched terrain [*Milam et al.*, 2003]. These images have not been radiometrically or geometrically calibrated. Craters C1 and C2 from Figure 13 are indicated for reference. (d) Inferred stratigraphy of Gusev crater where the etched layer is present. A thin surface mantle, tens of meters thick, locally overlies coarser (volcanic possibly overlying fluvial) materials that cannot be transported by wind.

Table 4. Estimated Volumes Discharged to Ma'adim Vallis From the Eastern, Northwest, and Southwest Paleolake Subbasins Filled to 1100 m and the Intermediate Basin Filled to 1000 m

Subbasin	Volume at 1,100 m or Full Level, km^3	Volume at 950 m Level or When Isolated, km^3	Volume Available for Discharge, km^3
Eastern subbasins	305,000	218,000 (at 950 m)	87,000
Northwest	58,000	48,000 (at 1035 m)	10,000
Southwest	139,000	122,000 (at 1050 m)	17,000
Intermediate basin	60,000 (at 1000 m)	0 (breached)	60,000
Total	562,000	388,000	174,000

lake initially occupied a uniform level of 1100 m, relative to present topography, and that the intermediate basin was initially dry. At this level, surface water would be available to Ma'adim Vallis from the eastern, northwestern, and southwestern subbasins (Figure 2). The southwestern subbasin would become isolated as the level declined below 1050 m, the northwestern subbasin would be closed at 1035 m, and the eastern subbasins alone would provide 87,000 km^3 of water to carve Ma'adim Vallis before the 950 m level was reached (Table 4). By this method, a total of 114,000 km^3 of water was delivered from the Eridania basin, consistent with a water/sediment volume ratio of 8:1 if a single flood excavated the total Ma'adim Vallis volume of 14,000 km^3. More conservatively, if contemporary topography was such that the three largest subbasins were not integrated at the time of the overtopping, and if the intermediate basin were initially dry, enough water was available in the eastern subbasins alone to carve Ma'adim Vallis, with a water/sediment ratio of at least 6:1 by volume, above the minimum ratio of 2.5:1 determined by *Komar* [1980].

[57] A more liberal estimate of flow volume assumes that the intermediate basin also contained a paleolake, with up to 60,000 km^3 of water below its 1000 m overflow level, and that the water level was as high as 1250 m in the eastern subbasins, relative to present topography. Adding this 150 m thick layer of water onto the 1100 m contour in the eastern subbasins (area ~625,000 km^2), yields an upper limit of 94,000 km^3 of additional water. Therefore, depending on assumptions, 87,000 to 268,000 km^3 of water was available to carve Ma'adim Vallis, yielding a reasonable water/sediment volume ratio on the order of ~10:1. Aquifer contributions may have also provided water to the eastern subbasins, extending the tail end of the flood.

4.2. Inner Channel Discharge

[58] As discussed in section 3.3, the discharge from the Eridania basin was likely variable during the overflow. Peak flood discharge calculations would have considerable error, as later incision of the inner channel has altered the geometry of Ma'adim Vallis, and stage indicators have not been observed for the peak flow when much of the excavation may have occurred. The inner channel is a more suitable site for discharge calculations, as the inner margins of the lower reach terraces provide an upper limit for the depth of confined flows. The nearly constant gradient of the lower reach (Figure 3) suggests that discharge was constant with distance from the head, consistent with a paleolake overflow. In channels where discharge increases with contributing area, the sediment transport capacity also increases with area, and progressively lower gradients are required in the down-valley direction to transport the load [*Gilbert*, 1877; *Davis*, 1902].

[59] *Cabrol et al.* [1998b] concluded that the wide Ma'adim Vallis floor was not a channel, because large flows were inconsistent with their interpretation of the valley's longevity. *Cabrol et al.* [1996] did, however, allow for some large discharges associated with the release of water from putative intravalley lakes. *Landheim* [1995] left open the possibility of a single large flow with later activity of tributaries. We find no compelling mechanism to explain the 3–5 km width of the valley floor unless a flow occupied its entire width. Fluvial dissection of the valley sidewalls was limited during and after incision of Ma'adim Vallis, in contrast to the Grand Canyon in the southwestern U.S., which is of similar size but has deeply dissected walls. This poor dissection makes it unlikely that water generated within the intermediate basin widened a narrow precursor Ma'adim Vallis over time to 15–25 km width. Few mass movements crosscut the usually shallow sidewall gullies, so postfluvial mass wasting does not explain the width, and furthermore the terraces and medial floor ridges are well preserved (Figures 14 and 15). The valley floor maintains much of its ~5 km width as it crosscuts impact crater rims, which are relatively resistant materials that have diverted the valley course somewhat in other locations (Figures 14 and 16c). Somewhat wider areas of the valley floor are associated with likely less resistant sedimentary materials, such as crater interior deposits (see C2 in Figure 16). Ma'adim Vallis narrows only where its slope increases, including along the upper reach and at the knickpoint, as expected for a channel that could freely adjust its cross-sectional area to suit a constant discharge and variable flow velocity. The western tributary is anastomosing without a sediment source above its head (Figure 4), suggesting a flow that the antecedent topography could not confine. The main valley and tributary are both ~3 km wide at their heads, unlike other valleys in the region. A layered medial bar at the confluence of the main valley and tributary stands ~120 m above the valley floor (Figure 15). The inner channel migrates to the outer margin of most bends in the valley's lower reach (Figure 13b), as expected for a channel incising along the thalweg of the terrace level (peak flood stage). Thalwegs are typically located along the outer margin of channel bends. The lower reach exhibits a step-pool sequence, with pools up to tens of meters deep (Figure 3b), which would require deep flows for excavation. The possible deltaic deposit in Gusev crater is small relative to the volume of Ma'adim Vallis (Figure 16b). Catastrophic floods typically do not leave deltas, as their velocities are adequate to maintain sediment transport well into the interior of their depositional basins, so the delta develop-

ment probably occurred only near the end of the flood. The low settling velocity on Mars relative to flow velocity [*Pieri*, 1980] would facilitate transport of suspended load into Gusev relative to a similar flow on Earth. The inner channel width is therefore likely related to the same flows that transported material through the valley.

[60] The above comparisons are qualitative, but we can test the paleolake overflow hypothesis by quantitatively comparing the inner channel of Ma'adim Vallis to terrestrial river channels. First, terrestrial river valleys have variable width/depth ratios, but an approximation can be made using empirical relationships between width W, depth H, and bankfull discharge Q_b (m^3/s) as

$$Q_b = (W/K_w)^2 = (H/K_h)^{2.8}, \quad (3)$$

where K_w and K_h are coefficients with one standard deviation ranges of 2.5–4.8 and 0.26–0.56, respectively [*Knighton*, 1987]. By taking the midpoints of these ranges, $K_w = 3.65$ and $K_h = 0.41$, a relationship between W and H can be determined:

$$H = 0.16W^{0.72}. \quad (4)$$

Equation (4) suggests that a channel 5 km wide should have a depth of approximately 70 meters, give or take a factor of ~2, so it would be ~70 times as wide as it is deep. The inner terrace margins, where scarps bound the inner channel, are as low as ~100 m above the valley floor and are appropriate to confine such a flow. Bend wavelength λ varies linearly with channel width as

$$\lambda = K_\lambda W, \quad (5)$$

where $K_\lambda \sim 7-14$. The shortest bend wavelength in Ma'adim Vallis is ~37 km, in the intermediate reach of the valley, so $K_\lambda > 7$, which is consistent with the range of λ/W observations from terrestrial channels. The interior floor of Ma'adim Vallis therefore has geometry consistent with a fluvial channel.

[61] Initial estimates of discharge were made using empirical relationships from terrestrial channels, where bankfull discharge (Q_b) is the dominant control on channel width [*Knighton*, 1998]. Here we make the assumption that a large flow could freely modify its channel banks, so a relationship between width and discharge would pertain to the inner channel of an entrenched valley [see *Montgomery and Gran*, 2001]. This assumption is supported by the nearly constant width of the inner channel. Discharge can be scaled to Mars using a unit-balanced version of equation (3) from stability analyses of terrestrial meandering rivers [*Anderson*, 1967; *Parker*, 1976], where K_w has units of $(s/m)^{0.5}$ and g and H are relative gravity and depth, respectively:

$$Q_b = \left(\frac{W}{K_w}\right)^2 (gH)^{1/2}. \quad (6)$$

Depth scales with the -0.23 power of gravity (G. Parker, University of Minnesota, personal communication, 2003), so $Q \approx 1 \times 10^6$ m^3/s. A combination of the Manning and continuity equations can also be used for a discharge estimate in channels that are much wider than deep, with the assumption of steady, uniform flow:

$$Q = H^{5/3} S^{1/2} g^{1/2} W n^{-1}, \quad (7)$$

where H is depth, S is slope (for the lower reach, $S = 0.0012$), g is relative gravity, and n is the Manning roughness coefficient. We assumed $n = 0.035$, comparable to that used by *O'Connor* [1993] for the Bonneville outflow. When combined with the gravitational scaling term in equation (7), this value of n is consistent with the results of *Wilson et al.* [2004] ($0.035/0.38^{1/2} = 0.0565$, much like their result of 0.0545), and the natural range of n would not alter the results by more than a factor of two in either direction. Discharge would be approximately $2-7 \times 10^6$ m^3/s for postulated flows of 50–100 meters deep. At the confluence of the main and large tributary valleys, a sedimentary bar is located within the channel, which also appears to have confined main valley flows. Using equation (7), we confirmed that a 5×10^6 m^3/s discharge would pass east of the bar, approaching the crest elevation without overtopping it.

[62] Finally, we used the step-backwater method [e.g., *Webb and Jarrett*, 2002; *Brunner*, 2002] to model flows of this order of magnitude, beginning with 30 cross sections along the lower reach. The computational procedure is as follows:

[63] 1. Assume a water surface and an appropriate discharge at the downstream cross section 1 and upstream cross section 2.

[64] 2. Measure hydraulic radius and cross-sectional area of the flow.

[65] 3. Calculate velocity (equation (8)), conveyance (equation (9)), and energy gradient (equation (10)).

[66] 4. Determine the energy loss between cross section 2 and cross section 1 (equations (11) and (12)).

[67] 5. Calculate the water surface elevation for the upstream cross section.

[68] 6. Vary the assumed upstream water surface iteratively to approach the calculated value.

[69] The inner margins of lower reach terraces, the medial bar elevation, and the empirical comparisons constrained the water surface elevation and discharge assumptions. For planetary applications, the step-backwater method suffers from poorly constrained estimates of water surface elevation and roughness, but the method can confirm that for a given roughness and discharge, the proposed channel is able to dissipate gravitational energy.

[70] Mean flow velocity V (m/s) is calculated from assumed Q and measured cross-sectional area A (m^2) by

$$V = Q/A. \quad (8)$$

The conveyance C is

$$C = (1/n) A R^{2/3} g^{1/2}. \quad (9)$$

where R (m) is the hydraulic radius ($R = A/P$ where P is the wetted perimeter). The energy gradient S between upstream (cross section 2) and downstream (cross section 1) points is

$$S = Q^2/C^2. \quad (10)$$

The energy equation predicts head losses between cross sections:

$$W_{S_2} + \frac{\alpha_2 V_2^2}{2g} = W_{S_1} + \frac{\alpha_1 V_1^2}{2g} + H_e, \quad (11)$$

where at the upstream cross section, W_{S2} is the water surface elevation, α_2 is a scaling coefficient assumed equal to 1 given no overbank flow, V_2 is mean velocity, and g is gravitational acceleration. The right side of the equation represents values for the downstream cross section, where H_e is energy head loss (m) between the sections:

$$H_e = LS + K_c\left(\frac{\alpha_2 V_2^2}{2g} - \frac{\alpha_1 V_1^2}{2g}\right), \quad (12)$$

L is the distance between cross sections (here 5 km, the approximate channel width), and K_c is an expansion or contraction loss coefficient, equal to 0.1 for contracting reaches or 0.3 for expanding reaches [*Brunner*, 2002].

[71] For modeled flows of $\sim 2 \times 10^6$ m^3/s, the lower reach geometry affords a reasonable energy head loss with distance, such that the predicted water surface increases at upstream cross sections, without requiring upstream declines in gradient to balance energy. At the steps in the lower reach (Figure 3b), the model fails as the Froude number F rises above one, where flow becomes supercritical (rapid) given these discharges.

$$F = V/(gH)^{1/2}. \quad (13)$$

The fact that the model predicts rapid flow at steps (followed by pools) in the longitudinal profile is another consistency with channel morphology created by a large discharge. It is important to note that these steps are likely not sapping headwalls. They are not scarps and do not appear in imaging, but are higher-than-average gradient reaches that were identified only in the topographic data. The succession of enclosed pools below these steps is inconsistent with origin by small flows. We did not model flow headward of the lower reach, as this discharge would become supercritical again over the knickpoint, and the upper reach lacks terraces to constrain the flow depth.

[72] Discharges of $1-5 \times 10^6$ m^3/s are on the low end of estimates for the Martian outflow channels (commonly 1–2 orders of magnitude greater) [*Carr*, 1979, 1996; *Baker*, 1982] and similar to the terrestrial Lake Missoula floods [*Baker*, 1982] and Athabasca Vallis [*Burr et al.*, 2002], but they are somewhat higher than the 1×10^6 m^3/s peak discharge calculated for the Lake Bonneville flood [*O'Connor*, 1993]. The Bonneville flood is a good example of an overflowing lake producing discharge on this order of magnitude, however. Peak discharge, at the terrace level of the Ma'adim Vallis lower reach, may have been considerably higher than this range. At a possible average 5×10^6 m^3/s, 87,000 to 268,000 km^3 of water would be discharged from the Eridania basin in ~201 to 620 days. The actual duration of the flood depends on precise knowledge of paleolake volumes and the change in discharge with time, but the flood may have lasted less than one Martian year. This estimate does not constrain the duration of low-discharge fluvial activity within Ma'adim Vallis, which was supplied mainly by the tributary network within and north of the intermediate basin. This later fluvial activity did not significantly modify the trunk valley shape or its interior landforms, however.

4.3. Sediment Transport

[73] The near-constant slope of the lower reach (~0.0012) and width of the inner valley (~5 km) suggest that Ma'adim Vallis was able to conform its channel geometry to flow conditions. This requires that the substrate be easily eroded by the available discharge, except at the knickpoint, where a likely bedrock outcrop resisted erosion. Sediment transport rates and the diameter of transportable particles are functionally related to bed shear stress τ (N/m^2),

$$\tau = \rho g R S, \quad (14)$$

where ρ is fluid density (kg/m^3). For $Q = 5 \times 10^6$ m^3/s, bed shear stresses on the order of ~400 N/m^2 are averages for the low-gradient intermediate and lower reaches. Pools would have lower shear stresses of 100–300 N/m^2, whereas shear stresses for steps, the steep upper reach and knickpoint (Figure 3) occupied the range of 500–1000 N/m^2. For the low-gradient reaches, particles <~1 cm diameter would be carried as suspended load, and particles as large as ~50 cm would be carried as bed load [*Komar*, 1980]. In high-gradient reaches, particles as large as one meter could be carried as bed load, although considerable uncertainty applies to the bed load/suspended load threshold for >10 cm particles [*Komatsu and Baker*, 1997]. With the flood able to move sediment of this size, only large bedrock blocks along the Ma'adim Vallis course would be able to resist the flow, which could otherwise modify its channel relatively freely.

[74] Presently, the channel floor is relatively flat in cross section along the lower reach. Steeper reaches of the channel, including the upper reach, knickpoint, and smaller steps, typically have concave-up floor cross sections. The knickpoint probably represents a bedrock outcrop, as its almost V-shaped cross section resembles that of terrestrial bedrock valleys. The overall form and longitudinal profile are very similar to knickpoints developed experimentally in uniformly moderately resistant material, where actual shear stress is only moderately greater than critical shear stress for erosion [*Gardner*, 1983]. Otherwise, Ma'adim Vallis appears to be incised into less well consolidated materials, including impact ejecta, megaregolith, and sedimentary deposits.

5. Post-Noachian Geomorphology

5.1. Eridania Basin

[75] Post-Noachian air fall materials profoundly affected the Eridania basin morphology, but cratered highland surfaces immediately to the north (and south of Medusae Fossae materials) were not significantly altered. The youngest of these materials is a ~1–10 m thick air fall deposit that mantles the impact-gardened surface south of ~35°S [*Mustard et al.*, 2001], including the southern portion of the Eridania basin. Partial deflation of this layer has created patches of smooth and pitted surfaces, which dominate the meter-scale surface texture where the deposit occurs (Figure 17). This layer is thought to have originated in the

last 10^5 years as ice-rich loess [*Mustard et al.*, 2001], with similar cycles of aeolian deposition and erosion extending over at least 10^6 to 10^7 years. By calculating differential slopes along MOLA data tracks, *Kreslavsky and Head* [2000] noted that mantling deposits had smoothed this region on 0.6 km length scales, but not adequately to modify roughness on 19.2 km scales, relative to equatorial highland topography. Mantling materials in this area were originally recognized by *Soderblom et al.* [1973] at kilometer resolution, coinciding approximately with the air fall materials identified in high-resolution imaging [*Mustard et al.*, 2001] and topography [*Kreslavsky and Head*, 2000].

[76] In the Eridania basin, the most significant of these layers is the Hesperian "Electris deposit" mapped by *Grant and Schultz* [1990], which overlies the southern margin of the Eridania basin watershed and parts of the basin floor (see their Figure 3). This layer is at least ~100–400 m thick, based on MOLA topographic profiles where its lower contact appears in crater walls or at the base of eroded scarps or mesas (Figure 18). As it mantles the Eridania basin and watershed surface irrespective of elevation, the Electris deposit is likely composed of air fall materials [*Grant and Schultz*, 1990]. The surface of the deposit appears durable at present, as it does not exhibit yardangs or other landforms attributable to aeolian deflation, and superposed valley networks often exhibit knickpoints where they compromise its surface. These valley networks are sparse, with broad undissected interfluves (Figure 18), in contrast to unmantled slopes north of ~30°S, where networks incised into older slopes are commonly denser. As erosion of the Electris material did not leave pedestal impact craters, *Grant and Schultz* [1990] concluded that the deposit was emplaced and partially stripped during a short interval, dated to the middle of the Hesperian period using N(5) crater counts.

[77] In the eastern subbasins, the air fall materials are often exposed as a scarp overlying the plains of the Eridania basin floor (Figure 18a). The deepest parts of the Eridania basin depressions may have experienced a late episode of lacustrine activity (or a terminal stage of the paleolake we discuss here) near the close of the Hesperian, when flat terraces were deposited around the center of the Gorgonum subbasin at a constant level of −300 m. These terraces overlie or onlap the eroded Gorgonum chaotic terrain mesas and maintain a pristine appearance [*Howard and Moore*, 2004]. Evidence for post-Hesperian aqueous processes is limited in this area. Very recent, fresh-appearing gullies occur along the sides of some chaotic terrain mesas, fresh crater walls, and graben in the Eridania basin [*Malin and Edgett*, 2000b], but these gullies are spatially confined and have not had much geomorphic effect. As Noachian surfaces are saturated with impact craters of ~40 m diameter, impact gardening has reworked all Noachian surfaces to at least ~8 m depth [*Hartmann et al.*, 2001] (Figure 12). This diffusive process would be effective at removing all Noachian landforms on the order of ~100 m width and

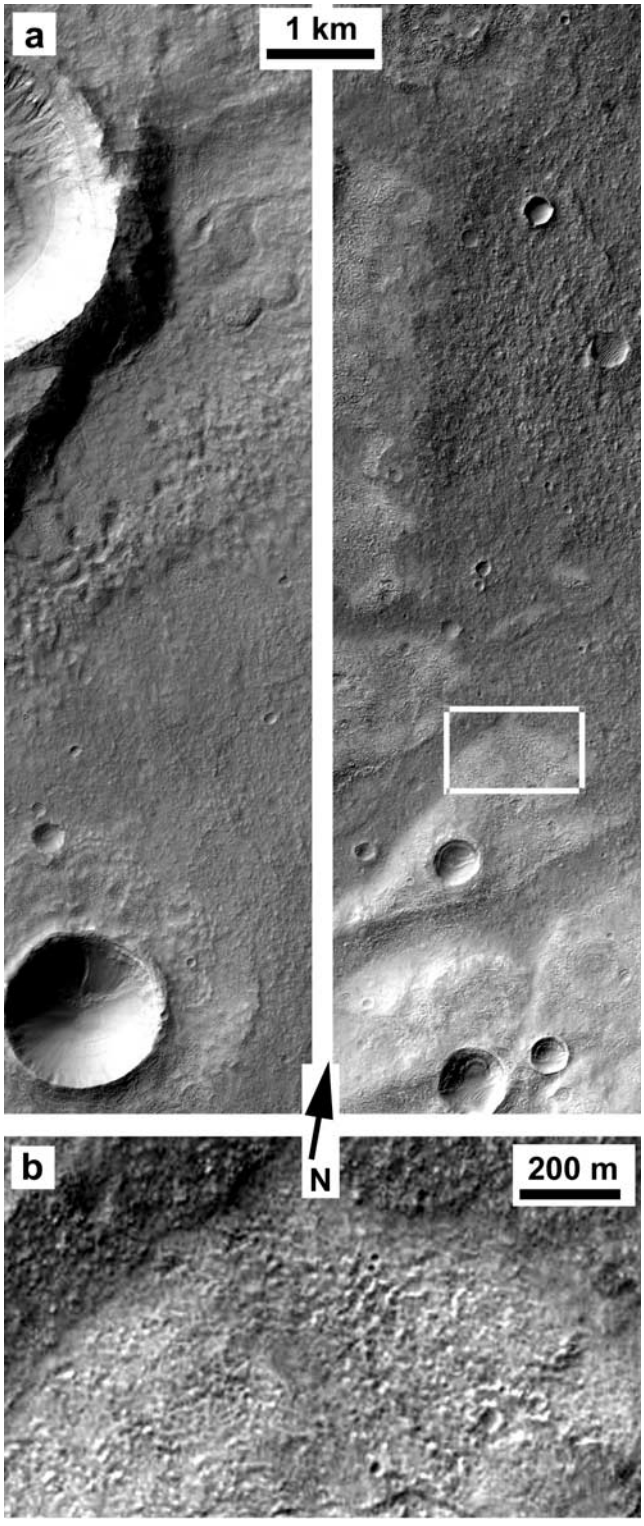

Figure 17. Subkilometer morphology in the Eridania basin south of ~35°S, representing post-Noachian resurfacing (subsets of MOC image M02-03267, centered at 39.18°S, 196.04°W). The left image is adjacent to and north of the right image. (a) Note the sparse small craters and rough, pitted surface, in contrast with the impact-gardened surface in Figure 12. Fresh gullies occur in some crater interiors, while older valleys are degraded where they debouched to the Eridania basin plains (bottom right). (b) Enlargement of white inset box in Figure 5a. The rough, pitted texture may be related to episodes of deposition and subsequent deflation of ice-rich loess [*Mustard et al.*, 2001], obfuscating any older, small-scale features.

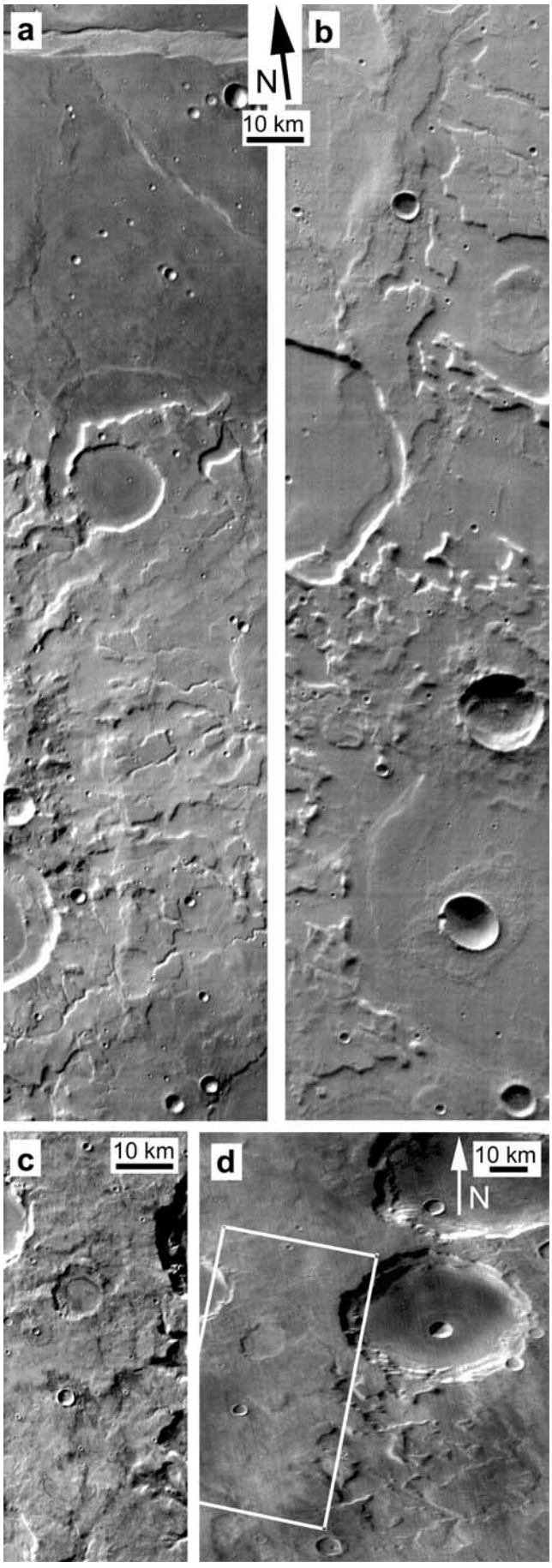

~10 m thickness. Tectonism also significantly modified the basin topography after the Noachian. In addition to the Sirenum Fossae and subperpendicular compressive ridges, circular ridges developed on the Eridania basin floor are thought to reflect compaction of plains over buried crater topography [*Watters*, 1993].

5.2. Ma'adim Vallis Watershed

[78] Longitudinal profiles of small Ma'adim Vallis tributaries (within the intermediate basin) suggest that fluvial activity modified the landscape somewhat, but not significantly, after the overflow. Where the surrounding terrain maintains adequately long and steep slopes, dense drainage networks exist down to the limit of THEMIS resolution (100 m/pixel; Figure 14) and extend to drainage divides, likely indicating that precipitation and runoff modified this landscape. Low-gradient surfaces are more commonly undissected over a range of elevations. Several of these tributaries have incised deep canyons along their lower reaches, which dissect the terraces and down-cut to the Ma'adim Vallis floor (Figure 14). This incision therefore postdates the complete incision of the main valley. At least three tributaries within the intermediate basin are hanging, in that they emerge well above the floor of the valley and exhibit a scarp but no incised knickpoint at the confluence. These tributaries, including the westernmost flood tributary course (the western point 3 in Figure 4a), are likely abandoned paleochannels that developed when the intermediate basin was draining, but before the intermediate reach was fully incised to its present level.

[79] Ideally, mature tributaries would develop graded (concave-up) longitudinal profiles where discharge increases with contributing area (i.e., in humid areas), such that downstream reaches have progressively greater discharge and can transport the sediment load under lower gradients [*Gilbert*, 1877; *Davis*, 1902]. The younger valley networks draining the intermediate basin (tributaries directly to

Figure 18. The ~100–400 m thick, Hesperian, Electris air fall deposit [*Grant and Schultz*, 1990] dominates kilometer-scale morphology along the southern margin of the Eridania basin watershed, where it has buried Noachian landforms. Note the relatively low density of small degraded craters and valley networks. (a) The margin of the deposit where it overlies the more durable ridged plains of the Eridania basin floor (subset of THEMIS daytime IR image I01168002, centered at 38.2°S, 174.5°E). Broad valleys were incised into the deposit, supplied by drainage from narrow upstream channels located atop the deposit. A Sirenum Fossae graben crosscuts the ridged plains at the top of the image. (b) More advanced erosion of the Electris deposit, where retreat of valley walls has isolated mesas (subset of THEMIS daytime IR image I03490002, centered at 38.8°S, 168.8°E). (c) Another example of narrow upstream valleys supplying broad lower reaches (subset of THEMIS daytime IR image I01168002, centered at 45.2°S, 173.5°E, located at the white inset box in Figure 18d). (d) The floor elevation of these broad reaches corresponds with terraces in nearby degraded crater walls, suggesting that the terraces reflect the base of weaker Electris materials (subset of MOC Geodesy Campaign Mosaic).

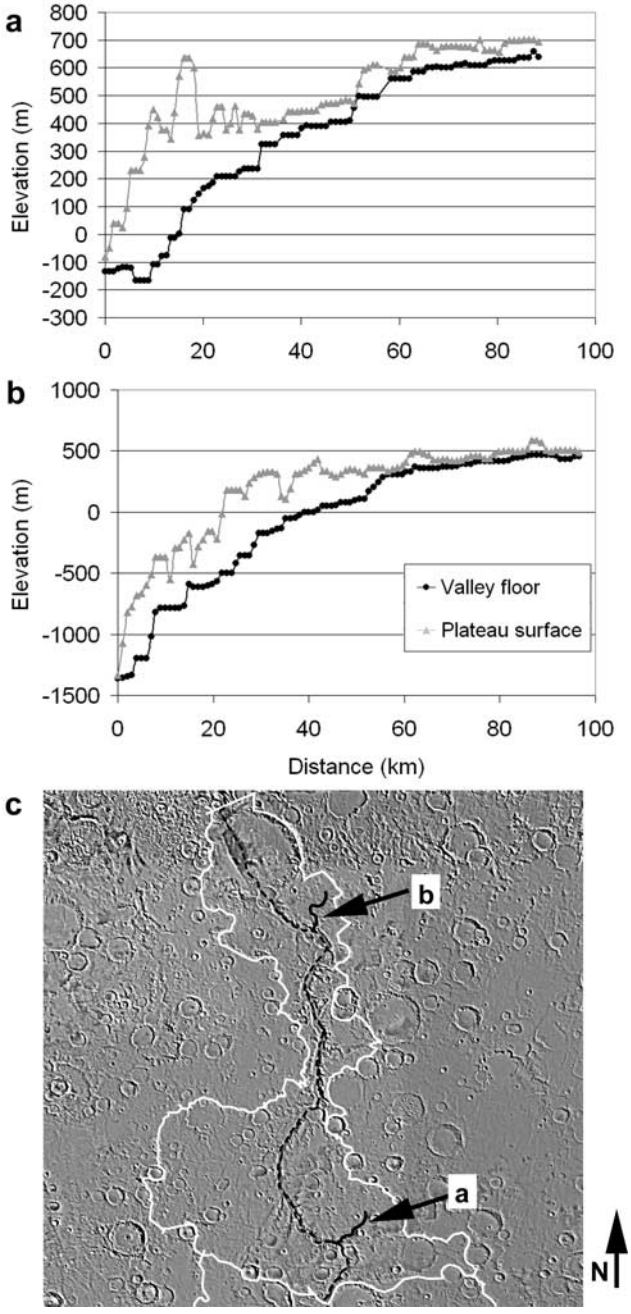

Figure 19. Typical convex-up longitudinal profiles of tributaries to Ma'adim Vallis. The tributaries become deeply incised only near the confluence with Ma'adim. In both cases, the channel "head" incises deeply into a plateau, but shallow contributing valleys are present upslope. Steps in the longitudinal profile appear where raw MOLA shots are not available; these are not real features of the valley. (a) Upstream tributary. (b) Downstream tributary. (c) Location of the tributaries (solid black lines). The dashed line is the Ma'adim main channel, and the white line is the drainage divide.

Ma'adim Vallis), in contrast, are poorly graded (Figure 19). The 17 tributaries we examined have convex-up longitudinal profiles, which commonly develop in fluvial systems in response to base level decline along the master stream. This is reasonable for Ma'adim Vallis if the valley incised rapidly relative to contemporary tributary incision rates, or if it was emplaced in a very short time with limited fluvial erosion afterward. These postflood tributaries may have supplied a small channel that is incised into the floor of Ma'adim Vallis near the mouth (across C1 in Figure 16c). This postflood small channel appears only near Gusev and is incised to below −1550 m, suggesting that the water level had by then declined in the crater.

6. Conclusions

[80] The excavation of Ma'adim Vallis, Mars, is best explained by (and probably requires) a catastrophic overflow of a ~1.1 M km^2 paleolake located south of the valley's source spillways. The paleolake overflow hypothesis is supported by the morphology and morphometry of Ma'adim Vallis and its head basin, flow modeling, and crater retention ages. This evidence includes the following:

[81] 1. Ma'adim Vallis originates at two incised gaps in the rim of a 500 km degraded crater, identified as the intermediate basin (Figure 1), which the valley crosscuts. The eastern source point, which is more deeply incised, is displaced ~25 km south of the original divide into the plains of the enclosed, 1.1×10^6 km^2 Eridania head basin. This displacement is consistent with terrestrial damburst floods and requires a large ponded water source within the Eridania basin. No sapping headwall, elevated aquifer, or contributing valley networks occur south of the valley heads, which are located at a topographic crest.

[82] 2. At its headward termination in the Eridania basin, Ma'adim Vallis has a floor width of 2.5–4 km, which is commensurate with downstream dimensions and suggests a large flow. The course of the western tributary is anastomosing, indicating that the landscape was unable to confine the large flows that breached the divide crest. The valley walls are poorly dissected, so water generated within the intermediate basin likely did not widen the valley over time, and postfluvial degradation processes have not substantially modified the valley's interior terraces and gullies.

[83] 3. Flow discharge was estimated by channel width and step-backwater modeling of a water surface below the inner margins of terraces, all of which yield discharges on the order of $1–5 \times 10^6$ m^3/s. A peak flood with greater discharge may have been responsible for eroding a wide valley at the terrace level before the inner channel was incised. Valley morphology and morphometry supports this use of the valley floor as a channel. All craters that have been breached by the valley have atypically wide gaps in their rims, as would be necessary to accommodate a large flow. Decreases in width are associated with increases in gradient. Interior ridges and a layered medial bar of 120 m height are consistent with flows that occupied the entire floor width. The width/depth ratio, width/bend wavelength ratio, and capacity to dissipate gravitational potential energy are consistent with terrestrial channels. The gradient of the lower reach is nearly constant, consistent with a constant discharge in the down-valley direction, with the exception of local steps and pools. The depth of these pools, up to tens of meters, suggests a deep flow.

[84] 4. When the topography of the region is reconstructed to before the incision of Ma'adim Vallis, the valley

course is shown to be entirely consistent with flow spilling over the preexisting landscape, exploiting low points in the topography and allowing the intermediate basin to be crosscut. No structural control of the valley course is evident.

[85] 5. The tributaries to Ma'adim Vallis are poorly graded to the main channel floor, as they have convex-up longitudinal profiles. These characteristics are consistent with rapid incision of the main valley relative to tributary incision rates, or a sudden incision of the valley followed by limited time for the adjustment of tributaries to the lowered base level.

[86] 6. The Eridania basin could contain adequate water (87,000 to 268,000 km^3) to erode the 14,000 km^3 volume of Ma'adim Vallis, with a physically plausible water-to-sediment volume ratio on the order of 10:1.

[87] 7. Crater counts suggest a similar age for the Eridania basin floor and for fluvial activity in the Ma'adim Vallis watershed (within the intermediate basin). Supported by other observations, the crater counts do not require the prolonged development of Ma'adim Vallis proposed by *Cabrol et al.* [1998b] and *Kuzmin et al.* [2000]. The paleolake overflow was contemporary with extensive fluvial erosion of the surrounding landscape, which probably required precipitation up to the Noachian/Hesperian boundary (using N(5)) [*Craddock and Maxwell*, 1990, 1993; *Grant*, 2000; *Craddock and Howard*, 2002; *Irwin and Howard*, 2002; *Hynek and Phillips*, 2003]. Since the Eridania basin is enclosed, lakes would be reasonable in the lower parts of the basin, which are the lowest areas on the Terra Cimmeria/Terra Sirenum plateau.

[88] 8. The Eridania basin contains six highly degraded impact craters of 180–240 km diameter with concave floors. Most Martian degraded craters have flat floors, which developed as the craters infilled [*Craddock and Maxwell*, 1993; *Craddock and Howard*, 2002], but the highly degraded Eridania basin depressions retain much of the craters' original interior relief. The topography of these depressions is similar to the other nearby large craters, Newton and Copernicus. The inward-sloping crater floors suggest a less efficient sediment transport process below ~700 m elevation, as occurs in standing water bodies. The relief in these concave crater floors is inconsistent with known volcanic surfaces on Mars, which are nearly flat or slope away from a central high point.

[89] 9. Nearly all valley networks in the Eridania basin watershed terminate between 1100 and ~700 m elevation, approximately 1 km above the low points in the respective drainage basins. The concave crater floors in the Eridania basin have slopes of ~0.5–1.5° below 700 m elevation, but the slopes are not dissected by valley networks. Similar slopes above 1100 m elevation are commonly dissected.

[90] 10. The boundary between the watershed and floor plains of the Eridania basin is similar to the elevation of the Ma'adim Vallis source breaches (~1100–1250 m), as might be expected for a paleolake surface.

[91] The Eridania basin's hypsometry and floor morphology suggest that a paleolake occupied temporally variable levels of 700–1250 m (modern topography may be somewhat modified by post-Noachian tectonism) during the time of widespread fluvial activity. The rims of large craters in the Eridania basin were extensively eroded above ~700 m, leaving large gaps in the rims, but topographic relief from 700 to −400 m lacks signs of incision and efficient sediment transport. We attribute the absence of valley networks in these crater floors to protection by standing water during the time that relatively intense fluvial erosion occurred.

[92] The Ma'adim Vallis development can be summarized in discrete stages as follows:

[93] 1. Near the Noachian/Hesperian boundary (using >5 km craters), water levels in the Eridania basin rose due to increased precipitation, reduced evaporation, and/or influx of groundwater from melting circumpolar ice or snow. A short-lived, contemporary lake may have formed in the intermediate basin.

[94] 2. The Eridania basin overflowed to the intermediate basin at two points at ~1200 to 1250 m elevation. The two-point overflow was possible because the original gaps likely had similar levels, and because available water from the $2–3 \times 10^6$ km^2 Eridania drainage basin exceeded the ability of either of the outlets (which were not yet fully incised) to discharge it. An impact into the lake may have facilitated breaching of the divide at two locations. Early in the flood, standing water protected the intermediate basin interior, so only limited incision of the upper reach occurred before the lower reach was incised.

[95] 3. The intermediate basin overflowed at ~1000 m elevation, and the lower reach of Ma'adim Vallis was incised to the terrace level (~−500 m), below the level of the intermediate basin floor (400 m). The intermediate reach of the main valley and the lower reaches of the western tributary were then incised.

[96] 4. Incision of the eastern outlet resulted in abandonment of the western outlet. Continued flows predominantly from the eastern outlet incised a constant-width inner channel in the lower reach that matches the width of the intermediate and upper reaches. This late stage discharge was $\sim 1–5 \times 10^6$ m^3/s. The upper reach of the main channel was fully incised to its present 950 m spillway, while the western tributary, having been abandoned, did not incise to the same extent. When the Eridania basin water declined to this level, the flow terminated.

[97] 5. After the flood ceased, drainage networks reactivated in the intermediate basin as tributaries to Ma'adim Vallis. Overall dissection of the Ma'adim Vallis walls was temporally limited, so that terraces and interior flow features are well preserved, and the tributaries are poorly graded to the main valley floor.

[98] 6. The Eridania basin paleolake level declined, and the 100–400 m thick Hesperian Electris air fall deposit [*Grant and Schultz*, 1990] was deposited along much of the Eridania basin floor and the southern margin of its watershed. Hesperian valley networks dissected the Electris deposit, which was then deflated from much of the Eridania basin floor. Subsequent impact gardening and thinner air fall deposits [*Mustard et al.*, 2001] dominate the present morphology of the Eridania basin.

[99] **Acknowledgments.** We gratefully acknowledge the constructive dialogue and support from Bob Craddock, John Grant, and Tom Watters. Ken Tanaka and Robert Brakenridge provided valuable reviews that improved the manuscript, although Brakenridge prefers a mechanism to form the valley involving a significant role for tectonism. The first author thanks Clyde Brown for assistance with field work at Lawn Lake. This

project was supported by a NASA Mars Data Analysis Program grant to Maxwell and a Planetary Geology and Geophysics grant to Howard.

References

Aharonson, O., M. T. Zuber, D. H. Rothman, N. Schorghofer, and K. X. Whipple (2002), Drainage basins and channel incision on Mars, *Proc. Natl. Acad. Sci U. S. A.*, *99*, 1780–1783.

Anderson, A. G. (1967), On the development of stream meanders, paper presented at 12th Congress of the International Association for Hydraulic Research, Fort Collins, Colorado.

Anderson, R. C., J. M. Dohm, M. P. Golombek, A. F. C. Haldemann, B. J. Franklin, K. L. Tanaka, J. Luis, and B. Peer (2001), Primary centers and secondary concentrations of tectonic activity through time in the western hemisphere of Mars, *J. Geophys. Res.*, *106*, 20,563–20,585.

Baker, V. R. (1982), *The Channels of Mars*, Univ. of Tex. Press, Austin.

Barlow, N. G. (1990), Constraints on early events in Martian history as derived from the cratering record, *J. Geophys. Res.*, *95*, 14,191–14,201.

Brakenridge, G. R. (1990), The origin of fluvial valleys and early geologic history, Aeolis quadrangle, Mars, *J. Geophys. Res.*, *95*, 17,289–17,308.

Brunner, G. W. (2002), *HEC-RAS River Analysis System Hydraulic Reference Manual, Version 3.1, CPD-69*, Hydrol. Eng. Cent., U.S. Army Corps of Eng.

Burr, D. M., J. A. Grier, A. S. McEwen, and L. P. Keszthelyi (2002), Repeated aqueous flooding from the Cerberus Fossae: Evidence for very recently extant, deep groundwater on Mars, *Icarus*, *159*, 53–73.

Cabrol, N. A., and E. A. Grin (1999), Distribution, classification, and ages of Martian impact crater lakes, *Icarus*, *142*, 160–172.

Cabrol, N., R. Landheim, R. Greeley, and J. Farmer (1994), Fluvial processes in Ma'adim Vallis and the potential of Gusev crater as a high priority site (abstract), *Proc. Lunar Planet. Sci. Conf. 25th*, 213–214.

Cabrol, N. A., E. A. Grin, and G. Dawidowicz (1996), Ma'adim Vallis revisited through new topographic data: Evidence for an ancient intravalley lake, *Icarus*, *123*, 269–283.

Cabrol, N. A., E. A. Grin, and G. Dawidowicz (1997), A model of outflow generation by hydrothermal underpressure drainage in volcano-tectonic environment, Shalbatana Vallis (Mars), *Icarus*, *125*, 455–464.

Cabrol, N. A., E. A. Grin, R. Landheim, R. O. Kuzmin, and R. Greeley (1998a), Duration of the Ma'adim Vallis/Gusev crater hydrogeologic system, Mars, *Icarus*, *133*, 98–108.

Cabrol, N. A., E. A. Grin, and R. Landheim (1998b), Ma'adim Vallis evolution: Geometry and models of discharge rate, *Icarus*, *132*, 362–367.

Cabrol, N. A., E. A. Grin, and W. H. Pollard (2000), Possible frost mounds in an ancient Martian lake bed, *Icarus*, *145*, 91–107.

Carr, M. H. (1974), The role of lava erosion in the formation of lunar rilles and Martian channels, *Icarus*, *22*, 1–23.

Carr, M. H. (1979), Formation of Martian flood features by release of water from confined aquifers, *J. Geophys. Res.*, *84*, 2995–3007.

Carr, M. H. (1996), *Water on Mars*, Oxford Univ. Press, New York.

Carr, M. H. (2002), Elevations of water-worn features on Mars, *J. Geophys. Res.*, *107*(E12), 5131, doi:10.1029/2002JE001845.

Carr, M. H., and G. D. Clow (1981), Martian channels and valleys: Their characteristics, distribution, and age, *Icarus*, *48*, 91–117.

Carter, B. L., H. Frey, S. E. H. Sakimoto, and J. Roark (2001), Constraints on Gusev basin infill from the Mars Orbiter Laser Altimeter (MOLA) topography, *Proc. Lunar Planet. Sci. Conf. 32nd*, abstract 2042.

Clifford, S. M., and T. J. Parker (2001), The evolution of the Martian hydrosphere: Implications for the fate of a primordial ocean and the current state of the northern plains, *Icarus*, *154*, 40–79.

Cohen, A. S. (2003), *Paleolimnology: The History and Evolution of Lake Systems*, 500 pp., Oxford Univ. Press, New York.

Craddock, R. A., and A. D. Howard (2002), The case for rainfall on a warm, wet early Mars, *J. Geophys. Res.*, *107*(E11), 5111, doi:10.1029/2001JE001505.

Craddock, R. A., and T. A. Maxwell (1990), Resurfacing of the Martian highlands in the Amenthes and Tyrrhena region, *J. Geophys. Res.*, *95*, 14,265–14,278.

Craddock, R. A., and T. A. Maxwell (1993), Geomorphic evolution of the Martian highlands through ancient fluvial processes, *J. Geophys. Res.*, *98*, 3453–3468.

Craddock, R. A., R. Greeley, and P. R. Christensen (1987), Martian outflow channels: IRTM and visual observations (abstract), *Proc. Lunar Planet. Sci. Conf. 18th*, 203–204.

Craddock, R. A., T. A. Maxwell, and A. D. Howard (1997), Crater morphometry and modification in the Sinus Sabaeus and Margaritifer Sinus regions of Mars, *J. Geophys. Res.*, *102*, 13,321–13,340.

Currey, D. R. (1990), Quaternary palaeolakes in the evolution of semidesert basins, with special emphasis on Lake Bonneville and the Great Basin, U.S.A., *Palaeogeogr. Palaeoclimatol. Palaeoecol.*, *76*, 189–214.

Davis, W. M. (1902), Base-level, grade, and peneplain, in *Geographical Essays*, vol. 18, pp. 381–412, Ginn, Boston, Mass.

De Hon, R. A. (1977), Geologic map of the Eridania quadrangle of Mars, *U.S. Geol. Surv. Misc. Invest. Ser., Map I-1008*, scale 1:5M.

French, H. M. (1976), *The Periglacial Environment*, 309 pp., Addison-Wesley-Longman, Reading, Mass.

Gardner, T. W. (1983), Experimental study of knickpoint and longitudinal profile evolution in cohesive, homogeneous material, *Geol. Soc. Am. Bull.*, *94*, 664–672.

Garvin, J. B., S. E. H. Sakimoto, and J. J. Frawley (2003), Craters on Mars: Global geometric properties from gridded MOLA topography, in *6th International Conference on Mars*, abstract 3277, Lunar and Planet. Inst., Houston, Tex.

Gilbert, G. K. (1877), Report on the geology of the Henry Mountains, U.S. Geogr. Geol. Surv. Rocky Mountain Reg., U.S. Govt. Print. Off., Washington, D. C.

Goldspiel, J. M., and S. W. Squyres (1991), Ancient aqueous sedimentation on Mars, *Icarus*, *89*, 392–410.

Goldspiel, J. M., S. W. Squyres, M. A. Slade, R. F. Jurgens, and S. H. Zisk (1993), Radar-derived topography of low southern latitudes of Mars, *Icarus*, *106*, 346–364.

Golombek, M. P., et al. (2003), Selection of the Mars Exploration Rover landing sites, *J. Geophys. Res.*, *108*(E12), 8072, doi:10.1029/2003JE002074.

Grant, J. A. (2000), Valley formation in Margaritifer Sinus, Mars, by precipitation-recharged ground-water sapping, *Geology*, *28*, 223–226.

Grant, J. A., and C. Fortezzo (2003), Basin hypsometry on the Earth, Mars, and the Moon, in *6th International Conference on Mars*, abstract 3050, Lunar and Planet. Inst., Houston, Tex.

Grant, J. A., and P. H. Schultz (1990), Gradational epochs on Mars: Evidence from west-northwest of Isidis Basin and Electris, *Icarus*, *84*, 166–195.

Grant, J. A., and P. H. Schultz (1993), Degradation of selected terrestrial and Martian impact craters, *J. Geophys. Res.*, *98*, 11,025–11,042.

Grant, J. A., et al. (2004), Surficial deposits at Gusev crater along Spirit rover traverses, *Science*, *305*, 807–810.

Greeley, R., and J. E. Guest (1987), Geologic map of the eastern equatorial region of Mars, *U.S. Geol. Surv. Misc. Invest. Ser., Map I-1802-B*, scale 1:15M.

Greeley, R., R. O. Kuzmin, S. C. R. Rafkin, T. I. Michaels, and R. Haberle (2003), Wind-related features in Gusev crater, Mars, *J. Geophys. Res.*, *108*(E12), 8077, doi:10.1029/2002JE002006.

Grin, E. A., and N. A. Cabrol (1997), Limnologic analysis of Gusev crater paleolake, Mars, *Icarus*, *130*, 461–474.

Gulick, V. C. (2001), Origin of the valley networks on Mars: A hydrological perspective, *Geomorphology*, *37*, 241–268.

Hartmann, W. K., and G. Neukum (2001), Cratering chronology and the evolution of Mars, *Space Sci. Rev.*, *96*, 165–194.

Hartmann, W. K., J. Anguita, M. A. de la Casa, D. C. Berman, and E. V. Ryan (2001), Martian cratering 7: The role of impact gardening, *Icarus*, *149*, 37–53.

Head, J. W., III, and S. Pratt (2001), Extensive Hesperian-aged south polar ice sheet on Mars: Evidence for massive melting and retreat, and lateral flow and ponding of meltwater, *J. Geophys. Res.*, *106*, 12,275–12,299.

Howard, A. D. (1998), Long profile development of bedrock channels: Interaction of weathering, mass wasting, bed erosion, and sediment transport, in *Rivers Over Rock: Fluvial Processes in Bedrock Channels*, *Geophys. Monogr. Ser.*, vol. 107, edited by K. Tinkler and E. Wohl, pp. 297–319, AGU, Washington, D. C.

Howard, A. D. (2000), Ancient crater basins: A triad of morphologies, *Eos Trans. AGU*, *81*(48), Fall Meet. Suppl., abstract P62C-06.

Howard, A. D., and J. M. Moore (2004), Scarp-bounded benches in Gorgonum Chaos, Mars: Formed beneath an ice-covered lake?, *Geophys. Res. Lett.*, *31*, L01702, doi:10.1029/2003GL018925.

Howard, A. D., R. C. Kochel, and H. E. Holt (Eds.) (1988), *Sapping Features of the Colorado Plateau: A Comparative Planetary Geology Field Guide*, *NASA Spec. Publ., NASA SP-491*, 108 pp., NASA, Washington, D. C.

Howard, J. H. (1979), Geologic map of the Phaethontis quadrangle of Mars, *U. S. Geol. Surv. Misc. Invest. Ser., Map I-1145*, scale 1:5M.

Hynek, B. M., and R. J. Phillips (2003), New data reveal mature, integrated drainage systems on Mars indicative of past precipitation, *Geology*, *31*, 757–760.

Irwin, R. P., and A. D. Howard (2002), Drainage basin evolution in Noachian Terra Cimmeria, Mars, *J. Geophys. Res.*, *107*(E7), 5056, doi:10.1029/2001JE001818.

Irwin, R. P., T. A. Maxwell, A. D. Howard, R. A. Craddock, and D. W. Leverington (2002), A large paleolake basin at the head of Ma'adim Vallis, Mars, *Science*, *296*, 2209–2212.

Jankowski, D. G., and S. W. Squyres (1993), "Softened" impact craters on Mars: Implications for ground ice and the structure of the Martian regolith, *Icarus*, *106*, 365–379.

Jarrett, R. D., and J. E. Costa (1986), Hydrology, geomorphology, and dambreak modeling of the July 15, 1982 Lawn Lake dam and Cascade Lake dam failures, Larimer County, Colorado, *U. S. Geol. Surv. Prof.*, *1369*.

Knighton, A. D. (1987), River channel adjustment—The downstream dimension, in *River Channels: Environment and Process*, edited by K. S. Richards, pp. 95–128, Basil Blackwell, New York.

Knighton, D. (1998), *Fluvial Forms and Processes: A New Perspective*, Oxford Univ. Press, New York.

Komar, P. D. (1980), Modes of sediment transport in channelized water flows with ramifications to the erosion of the Martian outflow channels, *Icarus*, *42*, 317–329.

Komatsu, G., and V. R. Baker (1997), Paleohydrology and flood geomorphology of Ares Vallis, *J. Geophys. Res.*, *102*, 4151–4160.

Kreslavsky, M. A., and J. W. Head (2000), Kilometer-scale roughness of Mars: Results from MOLA data analysis, *J. Geophys. Res.*, *105*, 26,695–26,711.

Kuzmin, R. O., R. Greeley, R. Landheim, N. A. Cabrol, and J. D. Farmer (2000), Geologic map of the MTM -15182 and MTM -15187 quadrangles, Gusev crater—Ma'adim Vallis region, Mars, *U. S. Geol. Surv. Geol. Invest. Ser., Map I-2666*, scale 1:500K.

Landheim, R. (1995), Exobiology sites for Mars exploration and geologic mapping of Gusev crater-Ma'adim Vallis, M.S. thesis, 167 pp., Ariz. State Univ., Tempe.

Landheim, R., N. A. Cabrol, R. Greeley, and J. D. Farmer (1994), Stratigraphic assessment of Gusev crater as an exobiology landing site (abstract), *Proc. Lunar Planet. Sci. Conf. 25th*, 769–770.

Lucchita, B. K. (1982), Preferential development of chaotic terrains on sedimentary deposits, in *Reports of the Planetary Geology Program*, *NASA Tech. Memo., NASA TM-85127*, 235–236.

Lucchita, B. K., and J. Dembosky (1994), Scarp heights of Martian channels from shadow measurements (abstract), *Proc. Lunar Planet. Sci. Conf. 25th*, 811–812.

Malin, M. C. (1976), Age of Martian channels, in *Studies of Martian Geology*, Ph.D. dissertation, chap. 2, pp. 48–73, Calif. Inst. of Technol., Pasadena.

Malin, M. C., and M. H. Carr (1999), Groundwater formation of Martian valleys, *Nature*, *397*, 589–591.

Malin, M. C., and K. S. Edgett (2000a), Sedimentary rocks of early Mars, *Science*, *290*, 1927–1937.

Malin, M. C., and K. S. Edgett (2000b), Evidence for recent groundwater seepage and surface runoff on Mars, *Science*, *288*, 2330–2335.

Masursky, H., J. M. Boyce, A. L. Dial, G. G. Schaber, and M. E. Strobell (1977), Classification and time of formation of Martian channels based on Viking data, *J. Geophys. Res.*, *82*, 4016–4038.

Masursky, H., A. L. Dial Jr., and M. E. Strobell (1980), Martian channels—A late Viking view, in *Reports of the Planetary Geology Program*, *NASA Tech. Memo., NASA TM-82385*, 184–187.

Maxwell, T. A., and G. E. McGill (1988), Ages of fracturing and resurfacing in the Amenthes region, Mars, *Proc. Lunar Planet. Sci. Conf. 18th*, 701–711.

McCauley, J. F., M. H. Carr, J. A. Cutts, W. K. Hartmann, H. Masursky, D. J. Milton, R. P. Sharp, and D. E. Wilhelms (1972), Preliminary Mariner 9 report on the geology of Mars, *Icarus*, *17*, 289–327.

McGetchin, T. R., M. Settle, and J. W. Head (1973), Radial thickness variation in impact crater ejecta: Implications for lunar basin deposits, *Earth Planet. Sci. Lett.*, *20*, 226–236.

Milam, K. A., K. R. Stockstill, J. E. Moersch, H. Y. McSween Jr., L. L. Tornabene, A. Ghosh, M. B. Wyatt, and P. R. Christensen (2003), THEMIS characterization of the MER Gusev crater landing site, *J. Geophys. Res.*, *108*(E12), 8078, doi:10.1029/2002JE002023.

Milton, D. J. (1973), Water and processes of degradation in the Martian landscape, *J. Geophys. Res.*, *78*, 4037–4047.

Montgomery, D. R., and K. B. Gran (2001), Downstream variations in the width of bedrock channels, *Water Resour. Res.*, *37*, 1841–1846.

Moore, J. M., and A. D. Howard (2003), Ariadnes-Gorgonum knob fields of north-western Terra Sirenum, Mars, *Proc. Lunar Planet. Sci. Conf. 34th*, abstract 1402.

Mustard, J. F., C. D. Cooper, and M. K. Rifkin (2001), Evidence for recent climate change on Mars from the identification of youthful near-surface ground ice, *Nature*, *412*, 411–414.

Mutch, T. A., and E. C. Morris (1979), Geologic map of the Memnonia quadrangle of Mars, *U.S. Geol. Surv. Misc. Invest. Ser., Map I-1137*, scale 1:5M.

O'Connor, J. E. (1993), Hydrology, hydraulics, and geomorphology of the Bonneville Flood, *Spec. Pap. Geol. Soc. Am.*, *274*.

Parker, G. (1976), Cause and characteristic scales of meandering and braiding in rivers, *J. Fluid Mech.*, *76*, 457–480.

Phillips, R. J., M. T. Zuber, S. C. Solomon, M. P. Golombek, B. M. Jakosky, W. B. Banerdt, R. M. E. Williams, B. M. Hynek, O. Aharonson, and S. A. Hauck II (2001), Ancient geodynamics and global-scale hydrology on Mars, *Science*, *291*, 2587–2591.

Pieri, D. C. (1980), Geomorphology of Martian valleys, in *Advances in Planetary Geology*, *NASA Tech. Memo., NASA TM-81979*, 1–160.

Ritter, D. F., R. C. Kochel, and J. R. Miller (1995), *Process Geomorphology*, 3rd ed., McGraw-Hill, New York.

Schneeberger, D. M. (1989), Episodic channel activity at Ma'adim Vallis, Mars (abstract), *Proc. Lunar Planet. Sci. Conf. 20th*, 964–965.

Schultz, R. A., and K. L. Tanaka (1994), Lithospheric-scale bucking and thrust structures on Mars: The Coprates rise and south Tharsis ridge belt, *J. Geophys. Res.*, *99*, 8371–8385.

Scott, D. H., and K. L. Tanaka (1986), Geologic map of the western equatorial region of Mars, *U. S. Geol. Surv. Misc. Invest. Ser., Map I-1802-A*, scale 1:15M.

Scott, D. H., E. C. Morris, and M. N. West (1978), Geologic map of the Aeolis quadrangle of Mars, *U. S. Geol. Surv. Misc. Invest. Ser., Map I-1111*, scale 1:5M.

Sharp, R. P., and M. C. Malin (1975), Channels on Mars, *Geol. Soc. Am. Bull*, *86*, 593–609.

Soderblom, L. A., T. J. Kreider, and H. Masursky (1973), Latitudinal distribution of a debris mantle on the Martian surface, *J. Geophys. Res.*, *78*, 4117–4122.

Strom, R. G., S. K. Croft, and N. D. Barlow (1992), The Martian impact cratering record, in *Mars*, edited by H. H. Kieffer et al., pp. 383–423, Univ. of Ariz. Press, Tucson.

Tanaka, K. L. (1986), The stratigraphy of Mars, *Proc. Lunar Planet. Sci. Conf. 17th*, Part 1, *J. Geophys. Res.*, *91*(suppl.), E139–E158.

Tanaka, K. L. (1997), Sedimentary history and mass flow structures of Chryse and Acidalia Planitiae, Mars, *J. Geophys. Res.*, *102*, 4131–4149.

Thornhill, G. D., D. A. Rothery, J. B. Murray, A. C. Cook, T. Day, J. P. Muller, and J. C. Iliffe (1993a), Topography of Apollinaris Patera and Ma'adim Vallis: Automated extraction of digital elevation models, *J. Geophys. Res.*, *98*, 23,581–23,587.

Thornhill, G. D., D. A. Rothery, J. B. Murray, T. Day, A. C. Cook, J.-P. Muller, and J. C. Iliffe (1993b), Discharge rates in Ma'adim Vallis, Mars (abstract), *Proc. Lunar Planet. Sci. Conf. 24th*, 1429–1430.

Ward, W. R. (1992), Long term orbital and spin dynamics of Mars, in *Mars*, edited by H. H. Kieffer et al., Univ. of Ariz. Press, Tucson.

Watters, T. R. (1993), Compressional tectonism on Mars, *J. Geophys. Res.*, *98*, 17,049–17,060.

Webb, R. H., and R. D. Jarrett (2002), One-dimensional estimation techniques for discharges of paleofloods and historical floods, in *Ancient Floods, Modern Hazards: Principles and Applications of Paleoflood Hydrology*, *Water Sci. Appl.*, vol. 5, edited by P. K. House et al., pp. 111–125, AGU, Washington, D. C.

Wilson, L., G. J. Ghatan, J. W. Head III, and K. L. Mitchell (2004), Mars outflow channels: A reappraisal of water flow velocities from water depths, regional slopes, and channel floor properties, *J. Geophys. Res.*, *109*, E09003, doi:10.1029/2004JE002281.

A. D. Howard, Department of Environmental Sciences, University of Virginia, 291 McCormick Road, Clark Hall, P.O. Box 400123, Charlottesville, VA 22903, USA.

R. P. Irwin III and T. A. Maxwell, Center for Earth and Planetary Studies, National Air and Space Museum, Smithsonian Institution, MRC 315, Washington, DC 20013-7012, USA. (irwinr@nasm.si.edu)